Modeling, Design, Control and Validation of a Multiple-input DC-DC Converter Topology for Effective Renewable Energy Management

By

Hassan AboReada

A Thesis Submitted in Partial Fulfillment

of the Requirements for the Degree of

Master of Applied Science

in the

Faculty of Engineering and Applied Science
Department of Electrical, Computer, and Software Engineering
University of Ontario Institute of Technology

April, 2019

THESIS EXAMINATION INFORMATION

Submitted by: **Hassan Aboreada**

Master of Applied Science in **Electrical and Computer Engineering**

Thesis title: Modeling, Design, Control and Validation of a Multiple-input DC-DC Converter Topology for Effective Renewable Energy Management

An oral defense of this thesis took place on April 11, 2019 in front of the following examining committee:

Examining Committee:

Chair of Examining Committee	Dr. Walid Morsi Ibrahim
Research Supervisor	Dr. Sheldon S. Williamson
Research Co-supervisor	Dr. Vijay Sood
Examining Committee Member	Dr. Shahryar Rahnamayan
Examining Committee Member	Dr. Mohamed Youssef
External Examiner	Dr. Ibrahim Dincer, UOIT - FEAS

The above committee determined that the thesis is acceptable in form and content and that a satisfactory knowledge of the field covered by the thesis was demonstrated by the candidate during an oral examination. A signed copy of the Certificate of Approval is available from the School of Graduate and Postdoctoral Studies.

Abstract

Multiple-input DC/DC Converter Topology for Energy Management System

By Hassan AboReada

Multiple-input power converters are receiving significant research attention as they offer several advantages over conventional converters, specifically their ability to interface multiple energy sources of various kinds. Additionally, they have promising features such as less components, higher power density and centralized control.

A novel multiple-input single-output DC-DC converter topology is proposed for effective energy management. The topology is designed depending on the conventional structure of boost and buck converters and benefits greatly from this combination. Effective energy management strategy is used and a simple control system is introduced by utilizing voltage and current control.

The converter is simulated and implemented in hardware testing as a 300W system to confirm the performance and validation of the topology and it is capable of supplying constant output power through different input sources with any voltage variation. The results show a high performance and all of the operating modes have been investigated.

Acknowledgments

This research was supported by my supervisors, Dr. Sheldon S. Williamson and Dr. Vijay Sood. I am thankful for their guidance and support throughout the course of this work.

I am also grateful to my colleagues at UOIT in the STEER group that was created by Dr. Sheldon S. Williamson for their guidance in assisting me with support and knowledge to help me complete my work.

I would like to thank Dr. Sheldon S. Williamson for the knowledge, leadership and being a part of the STEER group. I would also like to thank my peers and friend at UOIT.

Contents

List of Figures

List of Tables

List of Abbreviations

EV	Electric Vehicle
FC	Fuel cell
FET	Field effect transistor
IC	Integrated circuit
HEV	Hybrid Electric Vehicle
MI	Multi input
MOSFET	Metal-Oxide-Semiconductor Field-Effect Transistor
MPPT	Maximum power point tracking
PID	Proportional-Integral-Derivative
PV	Photovoltaic
SOC	State of Charge

List of Symbols

C	Capacitance	F
D	Duty Cycle	%
E	Energy	J
F	Frequency	Hz
G	Irradiation	$^{W}/_{m^2}$
I	Current	A
L	Inductance	H
$\boldsymbol{\mu}$	Permeability of Free Space	$^{H}/_{M}$
P	Power	Watt
R	Resistance	Ω
fs	Switching Frequency	Hz
T	Temperature	°C
V	Voltage	V

Chapter 1
Introduction

1.1. The Historic and Futuristic Perspective

The DC-DC conversion technique [1] was established in the 1920s and was used for simple voltage conversion, acting as a voltage divider. However, this technique was only able to deliver an output voltage that was lower than the input voltage and with minimal efficiency. Continued research aims to find equipment that will change the voltage level of the DC source to another higher or lower voltage level. Initially, basic types of converters were used in industrial applications prior to the Second World War. However, research halted during the war but the applications were recognized. Technological developments following the war required low DC power supply, thus efforts were continued to develop the conversion techniques of DC-DC converters.

The demand for utilizing renewable energy sources has significantly increased due to many environmental factors such as pollution and global warming. Greenhouse gas emissions and pollutants are detrimental to the environment, thus renewable energy sources have generated significant interest for many industrial and commercial applications. DC-DC converters [2] have the ability to connect distribution generation units such as wind turbines, solar panels, batteries, fuel cells and micro turbines.

These converters can be used for several applications such as energy storage systems, electric vehicles (EV) and hybrid electric vehicles (HEV), micro grid and space power systems. So the need for distributing power to a variety of consumption loads whose voltage levels are different motivates the development of a supply

structure with multiple voltages. Different topologies have been proposed to combine different types of renewable energy sources, reduce the cost and size of the converter as well as increase efficiency. Multiple-input DC-DC topologies have developed very quickly to improve security of supply.

1.2. Motivation

Renewable energy resources are promising key energy sources for the future as they are determined to be one of the most effective and efficient solutions for reducing human dependency on fossil fuels and improving energy development strategies. Development in renewable energy presents many challenges as the development relies heavily on power systems. Thus, significant research has been carried out to design new DC-DC power conversion systems [3] that utilize several energy sources, which can achieve increased advantages through the characteristics of power systems.

New topologies have been proposed to deliver a controlled output for different applications. Multiple-input DC-DC converters [4] are now able to interface different levels of inputs and combine the advantages to supply different levels of outputs. Continued research looks to improve the efficiency, modularity, reliability, control complexity and cost effectiveness of these converters. However, no single topology can handle the entire list of proposed goals. Power conversion systems are in need of different topologies that can utilize different types of renewable energy sources while reducing the number of components and cost, while also maximizing the utilization factor and efficiency of the conversion.

Recent advancements in DC-DC power conversion [5] concern the effective renewable energy management using different converter structures with multiple-inputs. However, development of multiple-input DC-DC converters requires an efficient control system, which requires the complexity of the control algorithm to be reduced. New topologies that manage several renewable energy sources effectively will be the solution to obtaining a converter structure that is capable of handling many of the necessary improvement goals.

1.3. Scope of Thesis

The focus of this thesis is utilizing various energy sources (i.e. a battery) to obtain a regulated output power. It is expected to use one converter for multiple applications and, thereby, reduce the number of switching modes and the control complexity.

1.4. Objectives of Thesis

The objective of this thesis is to use a multiple-input single-output converter structure to provide both load and battery with energy at the same time through efficient energy management and with the advantage of having a simpler control system.

1.5. DC-DC Converters

DC-DC converters are used to change DC energy from one voltage level to another. A DC source cannot be stepped down or up unlike an AC source of with a transformer. Thus, a DC-DC converter is the equivalent of a transformer that performs the conversion with the highest possible efficiency. DC-DC converters have many properties that can be changed according to the structure of the circuit, such as: efficiency, flexibility, reliability, load transient response and ripple. The structure of the circuit depends on the operating conditions such as electrical, input and output specifications to satisfy all constraints (i.e…, cost, size).

There are two different categories of DC-DC converters, as shown in Table 1.1:

Table 1.1: DC-DC converters

Non-isolated	**Isolated**
Buck	Half-Bridge
Boost	Full-Bridge
Buck-boost	Forward
Cuk	Flyback
Zeta	Pushpull
Sepic	Boost Half- Bridge

Non-Isolated Converters

For non-isolated converters, the input and output terminals share a common ground. This converter configuration is commonly used when the change in voltage level is low. Non-isolated converters cannot withstand high electrical voltages.

Isolated Converters

In isolated converters, the input and output terminals are electrically separate. This configuration is commonly used for high isolation purposes, to produce high quality DC sources, blocking interference and noise.

Each category of converter [6], isolated and non-isolated, includes various sub-type converters that are suitable for certain applications. Some converter types such as the buck converter are used for stepping down voltage while the boost converter is used for stepping up voltage, while the buck-boost is used for either stepping up or down the voltage. The DC-DC converters (shown in Figure 1.1) are utilized for an assortment of applications including storage, electric motor drives, instrumentation, switch mode DC power supplies, industrial equipment, industries, communications and so on.

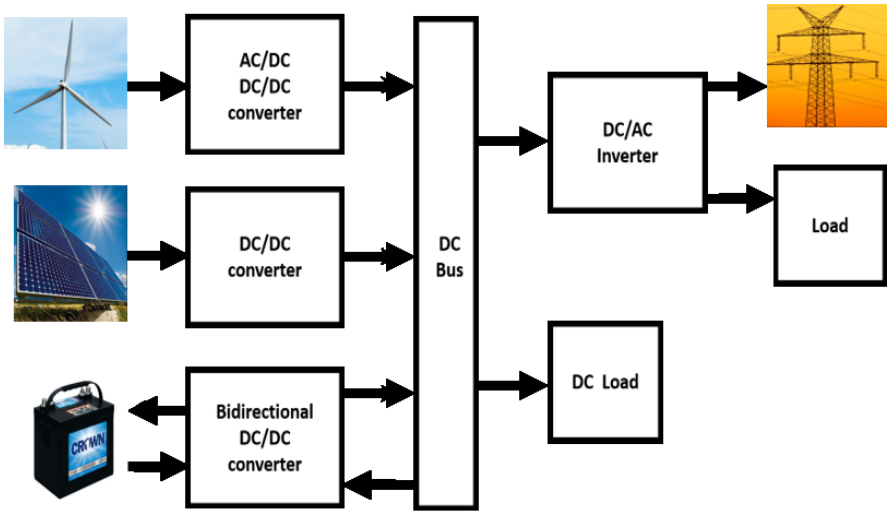

Fig 1.1: DC-DC converters and applications

DC-DC converters are power conversion circuits [7-8] were inductors, capacitors, frequency switching and transformers are used to reduce the switching noise for the regulated DC voltages. DC-DC converters depend on the switching mode which converts the DC voltage level by storing the input energy and then releases that energy at different output voltage. There are two types for such storage - magnetic field and/or electric field storage - and both depend on the utilization of various passive and active switching elements. For example, transformers and inductors are magnetic field components, capacitors are electric field components and power switches and diodes are switching elements.

The converter efficiency is increased by using power FETs which are able to switch with lower switching losses at high frequencies and have a low on resistance value. The basic design of converters is to go unidirectionally from input to output. But, by using independent control and replacing the diodes, it can go bidirectionally according to the switching topology. The magnetic field in the inductor stores and provides energy in a specific frequency range from 300 kHz to 10 MHz. The power delivered to the load is controlled by varying the duty cycle. This method can be applied to current and for having constant power.

The most important requirements for DC-DC converters are: high efficiency, good load transient response, small output ripple and stable operation. Good reliability and results can be achieved through reducing the failure rates and the impulse noises and switching time by selecting the maximum voltage and current values. The selection of switching frequency for the converter will influence the component selections in terms of electrical/thermal characteristics, physical size, frequency response and power losses. For example, high switching frequency will reduce the size of components such as capacitors, inductors,

resistors and transformers. Increasing the inductance value will increase the direct current resistance and the loss in case of heavy load.

The converter works in two ways: Stepping-up or stepping-down. Stepping-up the voltage will step-down the current and vice-versa. There is no ideal converter, but high efficiency can be achieved. The efficiency is given by:

$$\text{Efficiency} = {}^{P_{out}}/_{P_{in}} \tag{1.1}$$

The converter power flow is represented by the equation:

$$P_{in} = P_{out} + P_{loss} \tag{1.2}$$

Where P_{in} is the input power, P_{out} is the output power and P_{loss} is the power loss during the converter operation. To have an efficient converter without any losses, P_{out} should be equal to P_{in} by using the input voltage V_{in}, input current I_{in}, output voltage V_{out} and output current I_{out} as per the following equation:

$$V_{in} \times I_{in} = V_{out} \times I_{out} \quad \text{or} \quad {}^{V_{out}}/_{V_{in}} = {}^{I_{in}}/_{I_{out}} \tag{1.3}$$

Closed feedback loops are used to maintain constant output when there is a change in the input voltages and output currents values and they can achieve 90% or more efficiency but the problem is complexity and noise. DC-DC converter circuits have their unique switching frequencies which determine the efficiency and that affect the circuit properties as shown in Table 1.2:

Table 1.2: Relationships between efficiency and properties

Comparison	**High Efficiency**	**Low Efficiency**
Output current at maximum efficiency	Light load	Heavy load
Ripple	Large	Small
Response speed	Slow	Fast

1.6. Multiple-Input DC-DC Converters

Multiple-input (MI) DC-DC converter topologies [10] have the ability to combine several energy sources as shown in Figure 1.2 and consist of conventional DC-DC converter topologies. This combination provides some advantages according to the converter and the desired applications. The topology structure affects the cost and number of components, improves the reliability and efficiency of the overall system, reduces the control complexity and improves the energy management between all the available resources. They are categorized [11] into three groups:

- Magnetic: which includes topologies that have multi-winding transformer.
- Electrical: which consists of topologies that have DC-link and sources connected to the DC-link.
- Electro-magnetic: which includes topologies that have DC-link and two-winding transformer.

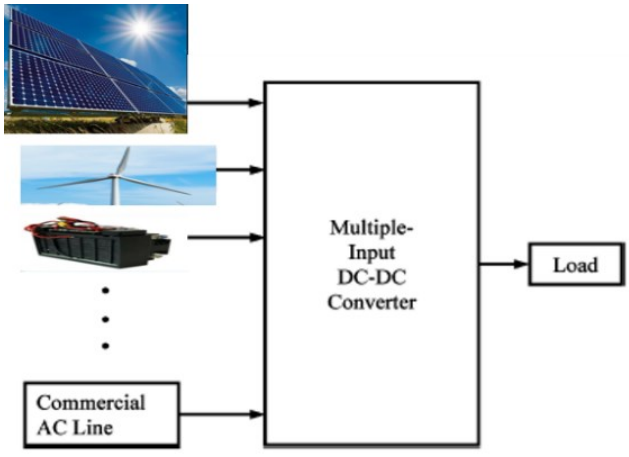

Fig 1.2: MI DC-DC converters

Multiple-input DC-DC converter [12] are known by having efficient power conversion and each one of them has their own structure, so they have notable advantages such as more efficiency and flexibility, less components, lower cost and better monitoring on the energy management resources. New topologies are proposed because of structure and characteristic benefits compared to the conventional converters as shown in Table 1.3.

Table 1.3: Conventional and MI converters comparison

Comparison	**Conventional**	**Multiport DC-DC Converter**
Number of power devices	More	Less
Control scheme	Separate control	Centralized control
Conversion stages	More	Less
Complexity	Structure-complex	Control-complex
Efficiency	Less	Improved

Chapter 2
Literature Review

The increased demand for utilizing several renewable energy sources with different input voltage levels presents new challenges in power conversion systems. Research on new topologies for multi-input DC-DC converters has gained significant interest and has become a large area of research. New control methods are implemented to improve the characteristics of the converter and different energy sources are used for better monitoring of energy management resources. A study has been done on the existing topologies to address the constraints and limitations of the converters, while taking into consideration the industrial growth in this area. The application requirements to obtain a new topology that combines several advantages and handles various applications is also taken into consideration.

2.1. Existing topologies

Existing topologies must be studied to determine the important constraints and advantages and to analyze the converter behavior and effectiveness of the control system. Six of the existing topologies are discussed next to provide an overview of the concept, operating modes and control system algorithm.

Multiple-input buck DC–DC converter

This topology [13] (Figure 2.1), utilizes two input sources and a battery. It consists of nine switching modes to control three states depending on a single inductor. It has only one single current sensor to monitor the gating signals of the switches.

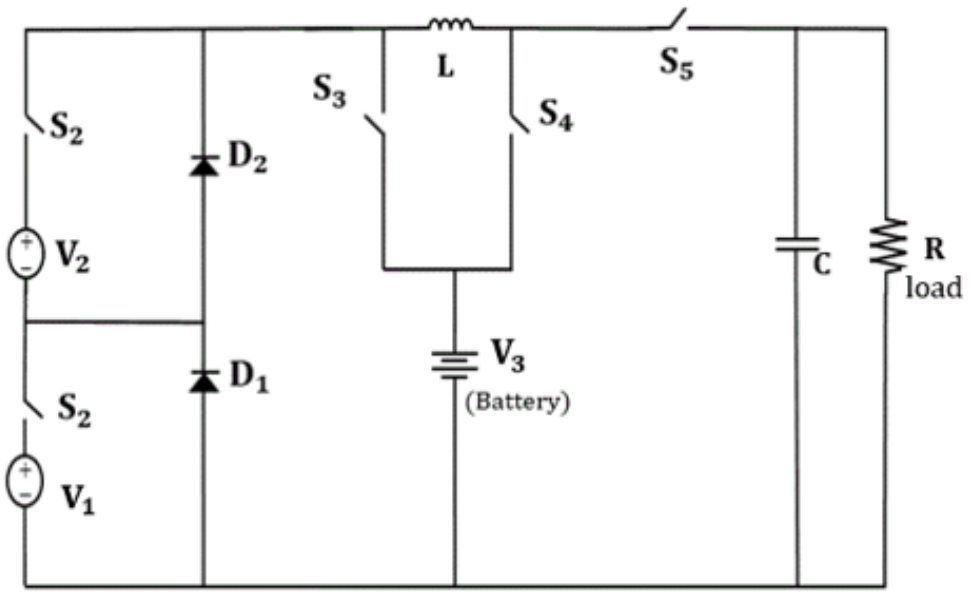

Fig 2.1: MI buck DC-DC converter topology

The three states are:

1. Charging the battery using one of the sources or both of them.
2. Supplying the load using one of the sources or both of them.
3. Discharging the battery to supply the load.

Benefits of the converter include smaller size, low cost, reduced mass and order reduction of the power conversion function. The control system of this converter relies on switching periods to extract more energy from the inputs by applying higher duty cycles for the input switches. The topology is designed for hybrid electric vehicle applications, as the output voltage is less than the minimum voltage and the power regulation capability is between the input and battery.

Three input DC–DC boost converter

This topology [14-15] (Figure 2.2), utilizes two input sources and a battery. It consists of 13 switching modes to control three different states and it depends on four different duty ratios to control the power switches. The states are:

1. Supplying the load through three switching modes.
2. Discharging the battery to supply the load through four switching modes.
3. Charging the battery through six switching modes.

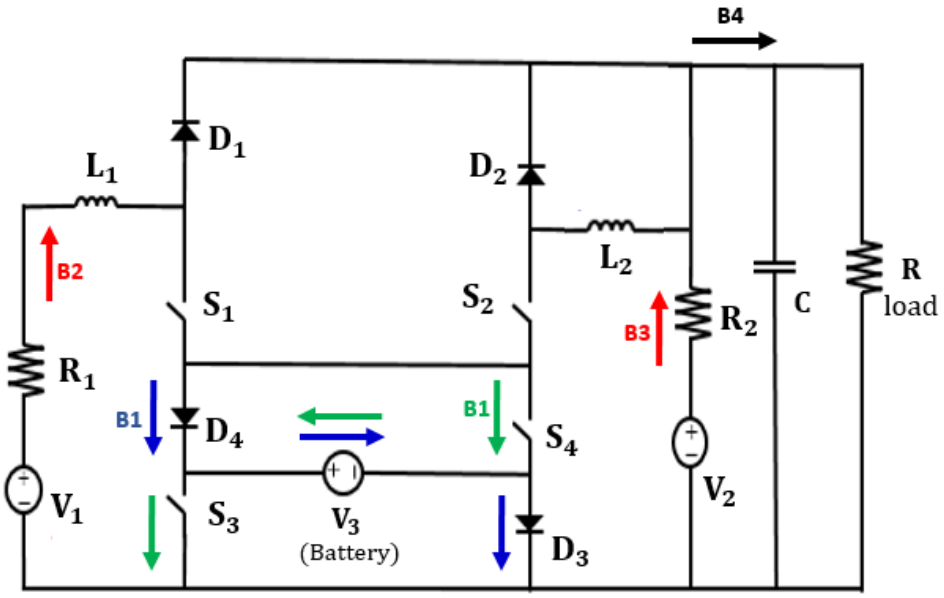

Fig 2.2: Three input DC-DC boost converter topology

This converter has four ports, one bidirectional port (B_1) for storage element, one port for output load (B_4) and two unidirectional ports (B_2, B_3) for input sources. The control system of this converter is relying upon decoupling network and closed-loop compensators to control the power flow among the input sources and the load and to step up the input voltages.

The topology is designed for hybrid power system applications and different energy sources can be utilized such as photovoltaic (PV) source, fuel cell (FC) source and battery.

Double input SEPIC/buck converter

This topology [16] (Figure 2.3), utilizes two input sources and consists of four operation modes and depends on two switches to supply the load. The topology is based on a buck and SEPIC converter. The converter introduces an enhancement of ripples in the current taken from the first source.

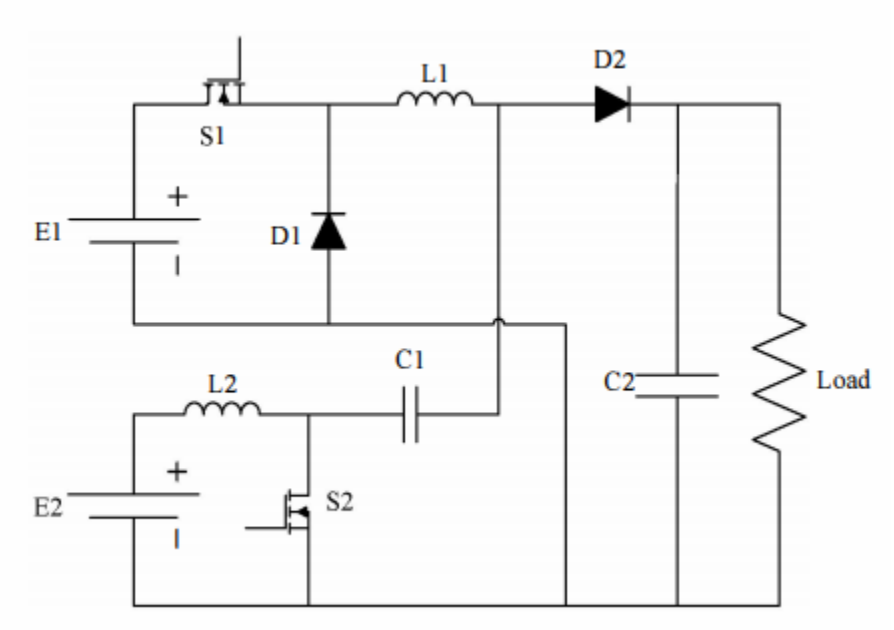

Fig 2.3: Double input SEPIC/buck converter topology

The operation modes are:

1. Supplying the load through the second source when S_1 and S_2 are off.
2. Supplying the load through the second source when S_1 is on and S_2 is off.
3. Supplying the load through the output capacitor when S_1 is off and S_2 is on.
4. Supplying the load through the output capacitor when S_1 and S_2 are on.

Multiple-input boost DC–DC converter

This topology [17] (Figure 2.4), utilizes two input sources and consists of four operation modes. It depends on a sliding mode control for better dynamic response and to avoid the utilization of current sensors. The converter is controlled in the voltage mode through two switches according to the availability of the voltage sources.

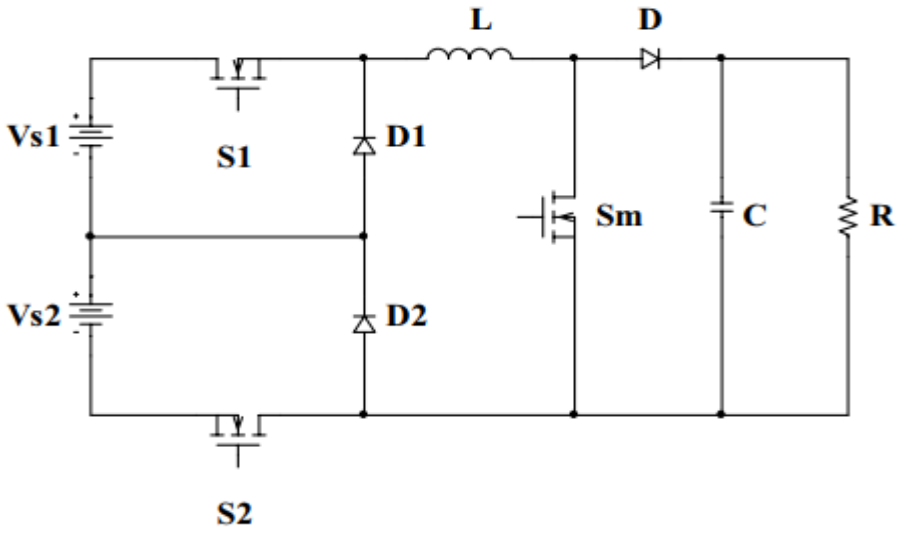

Fig 2.4: Multiple-input boost DC-DC converter topology

The operation modes are:

1. Supplying the load through the two sources and the ability of commutating S_1 and S_2 to deliver less energy.
2. Supplying the load through the first source if the second source is not available.
3. Supplying the load through the second source if the first source is not available.
4. Supplying the load through the free wheeling diodes using the remaining energy if the two sources are not available.

Buckboost-buckboost converter

This topology [18] (Figure 2.5), utilizes two input sources and consists of three operation modes and depends on two switches to supply the load as each source can supply the load individually or be supplemented with the stored energy in the inductor. The converter is not able to use two sources simultaneously.

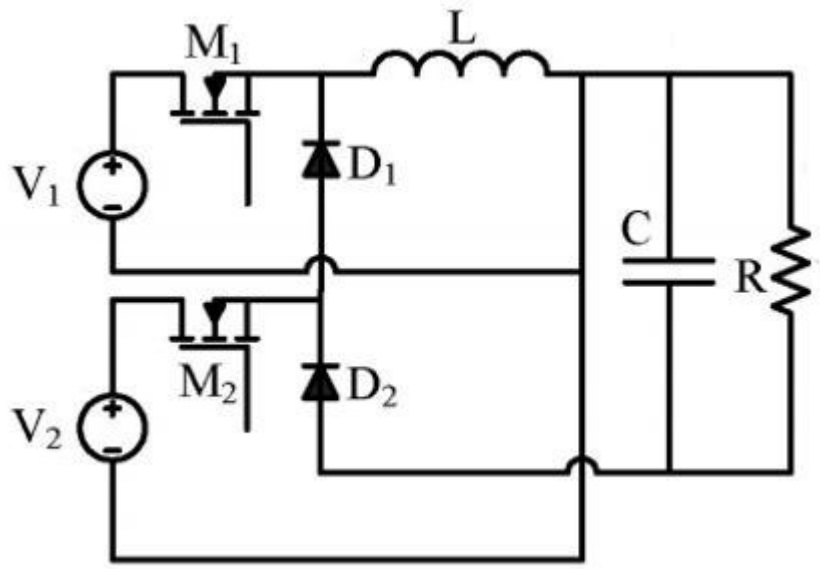

Fig 2.5: Buckboost-buckboost converter

The operation modes are:

1. Supplying the load through the first source V_1 when M_1 is on and M_2 is off.
2. Supplying the load through the second source V_2 when M_2 is on and M_1 is off.
3. Supplying the load through the output capacitor from the magnetic energy stored in the inductor as M_1 and M_2 are off.

Bridge-type multiple-input DC-DC converter

This topology [19] (Figure 2.6), utilizes two input sources and consists of three operation modes and depends on three switches to supply the load as each source can supply the load either individually or simultaneously. The power flow of the two sources to the load is managed by adjusting the duty cycles of the semiconductor switches (S_1, S_2 & S_3). The converter is designed for hybrid electric vehicle and renewable energy integration applications.

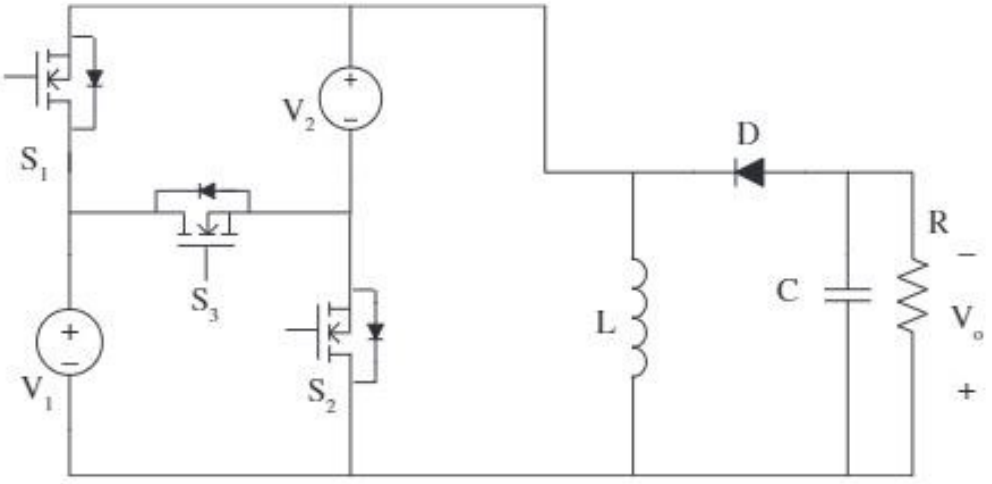

Fig 2.6: Bridge-type multiple-input DC-DC converter

The operation modes are:

1. Supplying the load through the first source V_1 when S_1 is on and S_2 and S_3 are off.
2. Supplying the load through the second source V_2 when S_2 is on and S_1 and S_3 are off.
3. Supplying the load through the two sources V_1 and V_2 when S_3 is on and S_1 and S_2 are off.

2.2. Challenges

Multiple-input DC-DC converters provide a unique solution to combine several input power sources with different voltage levels or power capacity to supply the load. They solved the sources connection problems of the conventional approaches. For the series connection of multiple sources, a control switch must be used for each voltage source to act as by-pass short circuit for input current of other supply. For the parallel connection, only one of the sources can be connected at a time because of the difference between the voltage amplitudes.

The most important constraints include: (a) inability of sources to supply the load constantly, (b) the control system depends on various switching periods or time sharing concept and (c) the power among different power ports cannot be transferred individually. Additional important constraints also include the lack of soft switching capability to allow high frequency design to further shrink the converter size, the large number of operation modes, utilization of the converter for only one specific application and the limitation of the converter as it cannot charge the battery or transfer energy into the load at once.

Chapter 3
Multiple-input, Single-output, Non-isolated DC-DC Converter

3.1. Introduction

This chapter discusses the circuit operation and control of the proposed converter for renewable energy applications. The topology is derived by combining buck and boost converters to provide a fixed output power to supply the load, with considerations of varying input voltages depending on smart energy management strategies. The converter is considered a non-isolated topology, which utilizes two energy sources to obtain regulated output power through the use of a battery as an additional source. The voltage levels of the source are distinctive, for example photovoltaic cells provide both the load and battery with energy simultaneously, through efficient power management and having the advantage of utilizing a simple topology structure. A simple control system is used with an efficient control algorithm to obtain a closed-loop controller design for the converter based on Proportional-Integral (PI) controllers. PI controllers were used to apply accurate and optimal control in terms of proportional, integral and derivative values, also to minimize the error over time. The PI controller was selected for its feasibility and easy implementation, as PI gains can be designed based on system parameters.

3.2. Circuit and Topology

As shown in Figure 3.1, the MI DC-DC converter uses the boost and buck structures and it has two different DC input sources which can be renewable energy sources, one battery, three inductors, two capacitors, two diodes, one resistance, six MOSFETS. There no limitations for the duty cycle as it can be changed depending on the voltage variation of the input sources in any of the operation modes in both boost and buck stages to get the desired fixed output power. The switching sequence ensures an energy management between all sources and maintains a longer life for the battery.

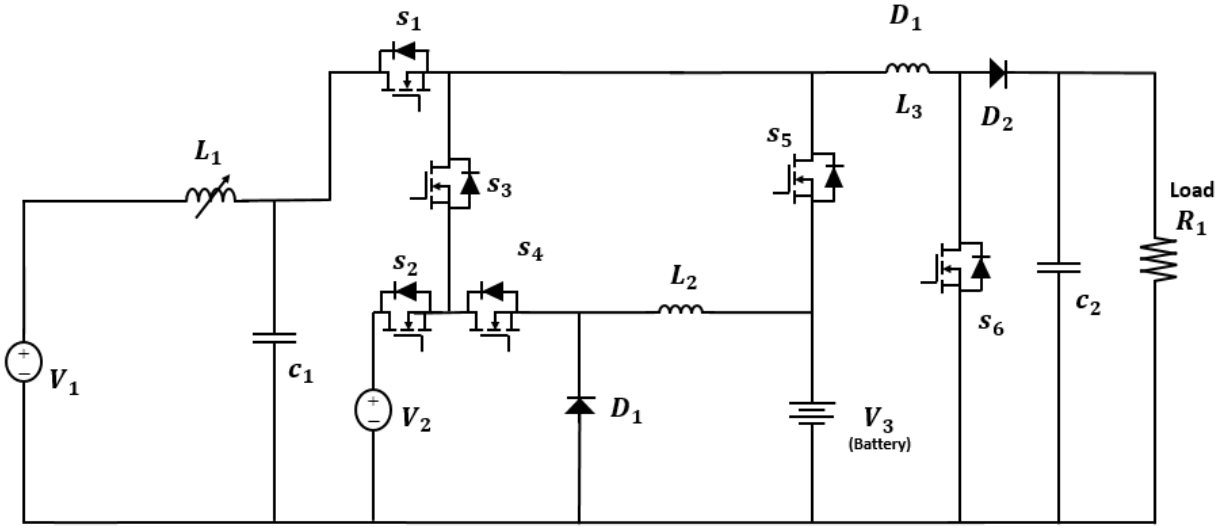

Fig 3.1: Multi-input, Single-output, Non-isolated DC-DC Converter

The switching sequence of the operational modes depends on specific consideration related to the input sources and the battery, as the maximum and minimum voltage values of the input sources have to be specified as well as the maximum and minimum values for the SOC of the battery. The circuit operation and the topology analysis will be discussed next.

3.2.1. Circuit Operation Principles

The switching modes of the converter are determined according to the input voltage and the state of charge (SOC) of the battery compared to a fixed value for both depending on the design and the application used, as shown in Table 3.1.

Table 3.1: Switching modes of the converter

Switching modes						
	S1	S2	S3	S4	S5	S6
Mode-1	ON	ON	OFF	ON	OFF	ON
Mode-2	ON	OFF	ON	ON	OFF	ON
Mode-3	ON	OFF	OFF	OFF	OFF	ON
Mode-4	OFF	OFF	OFF	OFF	ON	ON
1. Load supplying using V1 and battery charging mode using V2 2. Load supplying and battery charging mode using V1 3. Load supplying mode using V1 4. Load supplying and battery discharging mode						

The switching operation depends on two current sensors and one voltage sensor to obtain the desired duty cycle in each mode according to the input voltage and to operate in different modes which are: “Load supplying using V1 and battery charging mode using V2” or “Load supplying and battery charging mode using V1” or “Load supplying mode using V1” or “Load supplying and battery discharging mode”.

3.2.2.Converter Analysis

The converter is designed using the basic switching converter topologies for boost and buck converters. The design consists of number of storage elements and switches which are connected in a topology such that the periodic switching actions of the switches control the dynamic transfer power from the input to the output to produce a desired DC conversion at the output.

The boost stage provides an output voltage greater than the input voltage using a power MOSFET (S_6) as the switching transistor and the operation is divided into two modes depending on the switching actions of its switching transistor as shown in Figure 3.2.

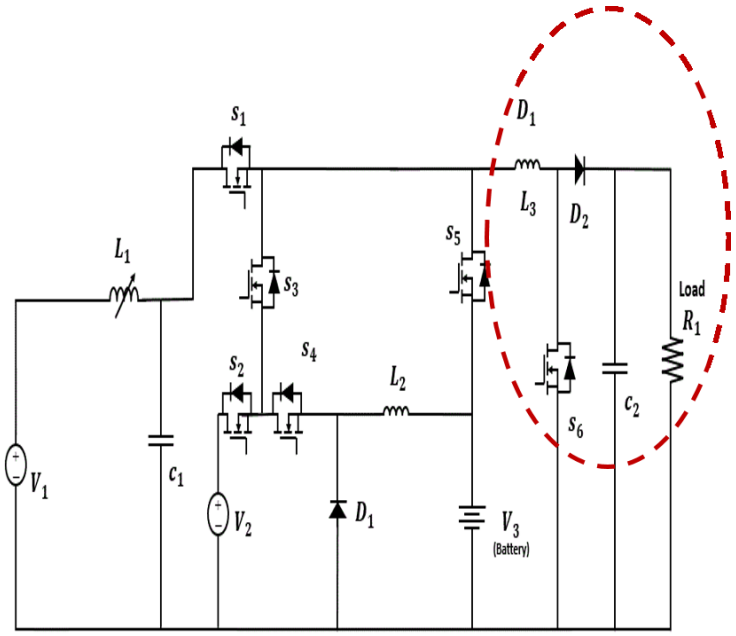

Fig 3.2: Boost stage

Mode I ($0 < t \leq t_{on}$): The switching transistor is switched at t=0 and it terminates at t = t_{on} and the diode is reverse biased since the voltage drop across the switching transistor is smaller than the output voltage.

The duration of t_{on} interval can be expressed as:

$$\mathrm{t_{on}} = \mathrm{L}\frac{\Delta I}{\mathrm{V_{in}}} \qquad (3.1)$$

The energy stored in the inductor is:

$$E = \frac{1}{2\mathrm{L}}\, {V_{in}}^2 {t_{on}}^2 \qquad (3.2)$$

The output current during this interval is supplied entirely from the output capacitor C, which is chosen to be large enough to supply the load current during the on time with a minimum specified droop in the output current.

Mode II ($t_{\mathrm{on}} < \mathrm{t} \leq \mathrm{T}$): The switching transistor is switched off at t= t_{on} and the voltage in the inductor reverses its polarity in an attempt to maintain a constant current as the current in the inductor cannot change instantaneously. The current that was flowing through the switching transistor will flow through inductor L, capacitor C, diode D and the load. The inductor current falls until the switching transistor is turned on again in the next cycle. The inductor delivers its stored energy to the capacitor C and charges it up through the diode to a higher voltage than the input voltage than the input voltage. This energy supplies the current and replenishes the charge drained away from the capacitor C when it alone was supplying the load current during the on time.

The duration of t_{off} interval can be expressed as:

$$\mathrm{t_{off}} = \mathrm{L}\frac{\Delta I}{\mathrm{V_o} - \mathrm{V_{in}}} \qquad (3.3)$$

The parameters of the boost stage can be determined according to the selected input and output voltage, voltage and current ripples and the switching frequency f_s. The parameters which are the inductor L, capacitor C and duty cycle can be calculated by using the following equations:

$$\frac{V_o}{V_{in}} = \frac{1}{1-D} \quad (3.4)$$

$$I_L = \frac{V_o\, I_o}{V_{in}} \quad (3.5)$$

$$\Delta V_0 = V_0(V_{ripple}) \quad (3.6)$$

$$\Delta IL = I_L(I_{ripple}) \quad (3.7)$$

$$C = \frac{(D)I_0}{f_s(\Delta V_0)} \quad (3.8)$$

$$L = \frac{(D)V_{in}}{f_s(\Delta IL)} \quad (2.9)$$

The buck stage provides an output voltage less than the input voltage and the operation is divided into two modes depending on the switching actions of its switching transistor (S_4) as shown in Figure 3.3.

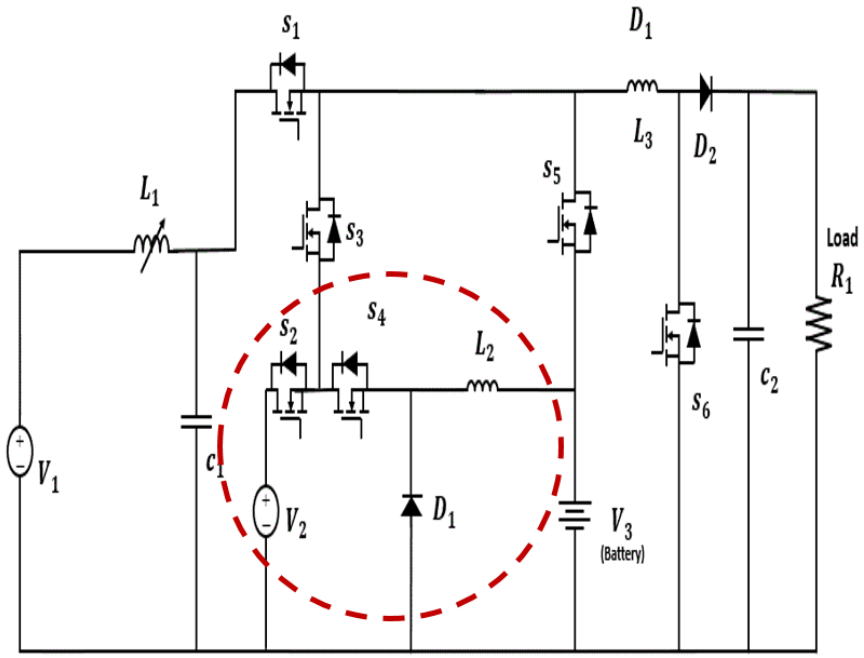

Fig 3.3: Buck stage

Mode I ($0 < t \leq t_{on}$): The switching transistor is switched at t=0 and the current in the inductor ramps upward during this interval, knowing that the voltage across the inductor L is related to the rate of rise of its current.

The duration of t_{on} interval can be expressed as:

$$t_{on} = L\frac{\Delta I}{V_{in} - V_o} \qquad (3.10)$$

So the first mode is characterized by the storage of energy in the magnetic field of the inductor.

Mode II ($t_{on} < t \leq T$): The switching transistor is switched off at t= t_{on} and the voltage polarity across the inductor immediately reverses trying to maintain the same current which had been flowing just prior to switching off of the switching transistor as the current in the inductor cannot change instantaneously.

The diode conducts since it is forward biased just as the inductor voltage reverses its polarity and the energy stored in the inductor supplies the load.
The duration of t_{off} interval can be expressed as:

$$\mathrm{t_{off}} = \mathrm{L}\frac{\Delta I}{\mathrm{V_o}} \qquad (3.11)$$

The parameters of the buck stage can be determined according to the selected input and output voltage, voltage and current ripple and the switching frequency $\mathrm{f_s}$. The parameters which are the inductor L and duty cycle can be calculated by using the following equations:

$$D = \frac{V_o}{V_{in}} \qquad (3.12)$$

$$\Delta V_0 = V_0(V_{ripple}) \qquad (3.13)$$

$$\Delta IL = I_o(I_{ripple}) \qquad (3.14)$$

$$L = \frac{(V_{in}-V_0)D}{f_s(\Delta IL)} \qquad (3.15)$$

The converter is designed to utilize two different renewable energy sources to make the converter more efficient for practical use for different applications, the two sources were considered to be implemented at different locations, so a parasitic inductance is added to take into account any time delays in response, as shown in Figure 3.4.

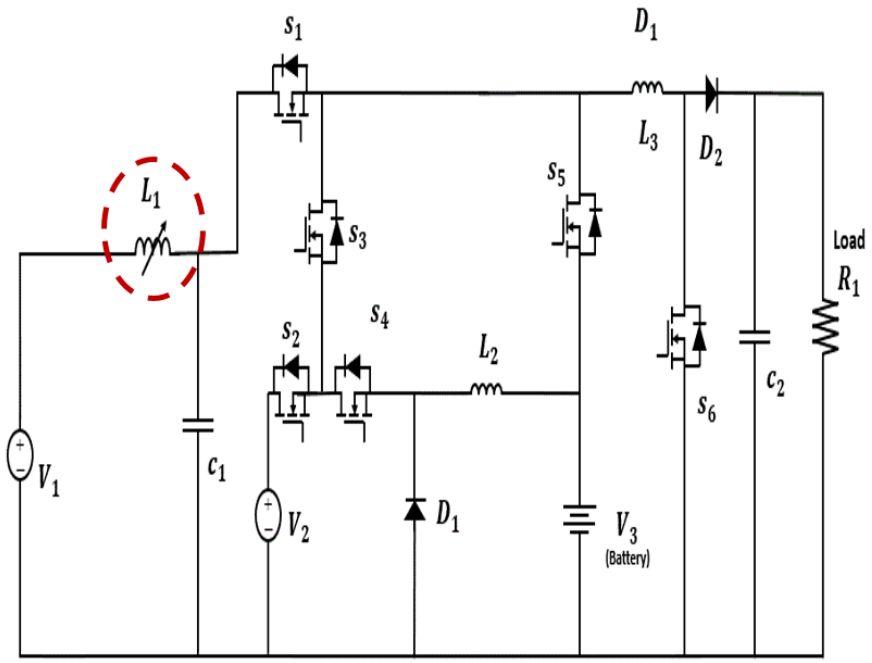

Fig 3.4: Parasitic inductance

The distance of the source estimated to be 500 m and the inductor value can be calculated by determining the values of the permeability of free space **μ**, number of turns **N**, length L and area A of the coil by using the following equation:

$$L = \frac{\mu N^2 A}{L} \qquad (3.16)$$

3.2.3. Mode Definition

There are four different operation modes controlled according to the input voltage level and the state of charge of the battery to obtain a fixed output power and to achieve an effective energy management of all the sources implemented to the converter.

Mode I (S_1, S_2, S_4 & S_6 : on): In this mode the two sources are working at the same time, V_1 supplies energy to inductor L_3 and the load and V_2 supplies energy to inductor $L_2$and the battery. There are two separate stages, boost stage and buck stage using the basic design of each one to ensure a high performance and each one operates with different duty cycle according to the voltage variation of input sources as shown in Figure 3.5.

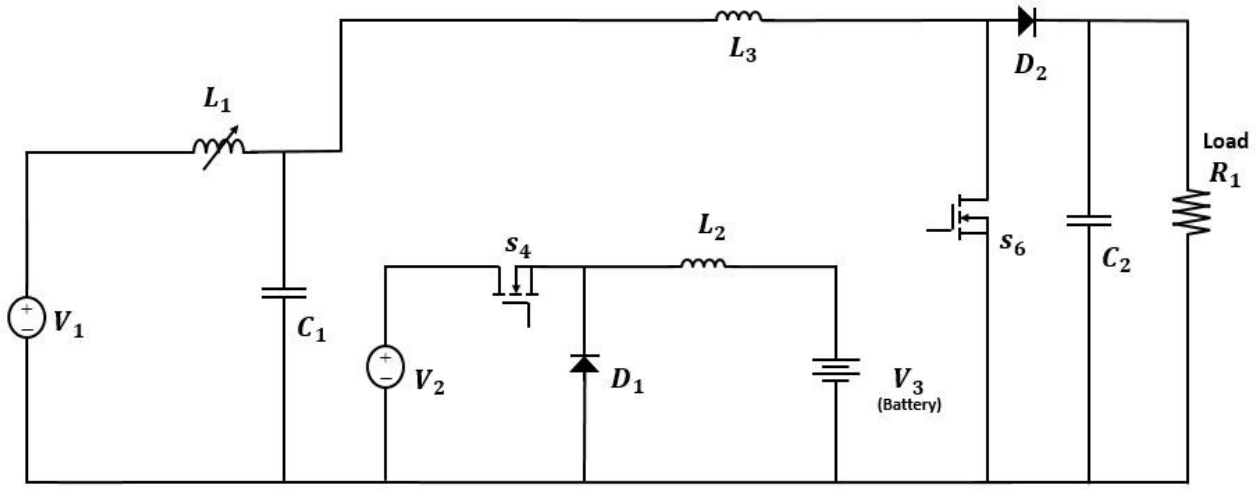

Fig 3.5: Mode I: Load supplying and battery charging mode through two sources

Mode II (S_1, S_3, S_4 & S_6 : on): In this mode one source is working as the other source cannot supply enough energy ($V_2 < V_{\min}$), V_1 supplies energy to inductors L_3 and L_2 , the load and the battery. The circuit combine between both boost and buck stages as $V_1$is the main source as shown in Figure 3.6.

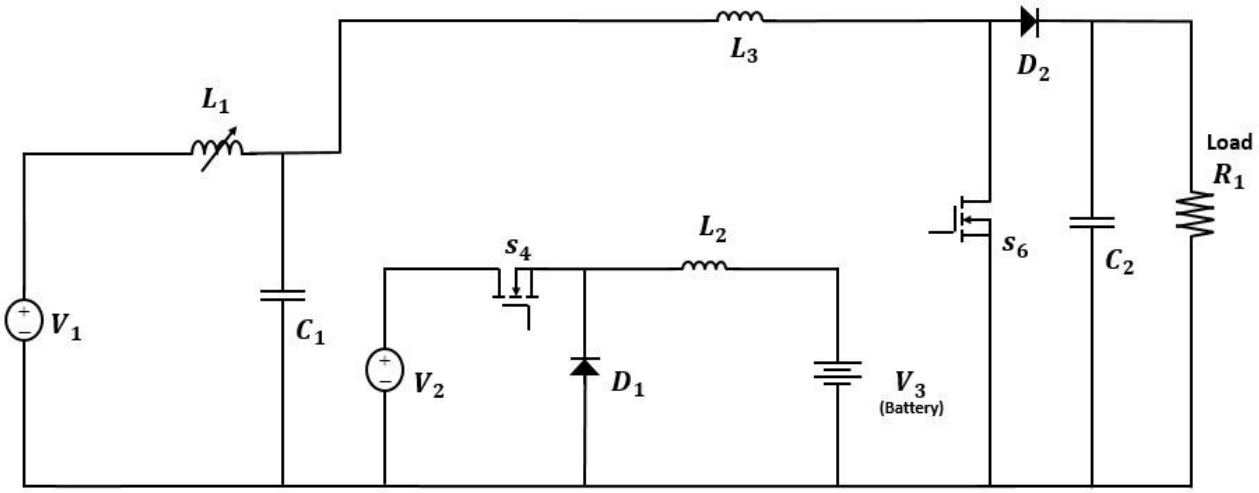

Fig 3.6: Mode II: Load supplying and battery charging mode through one source

Mode III (S_1 & S_6 : on): In this mode V_1 supplies energy to inductor L_3 the load as the SOC of the battery equal the SOC_{max} . There is only one stage which is the boost stage to supply the load as the second source is terminated to maintain the battery life time as shown in Figure 3.7.

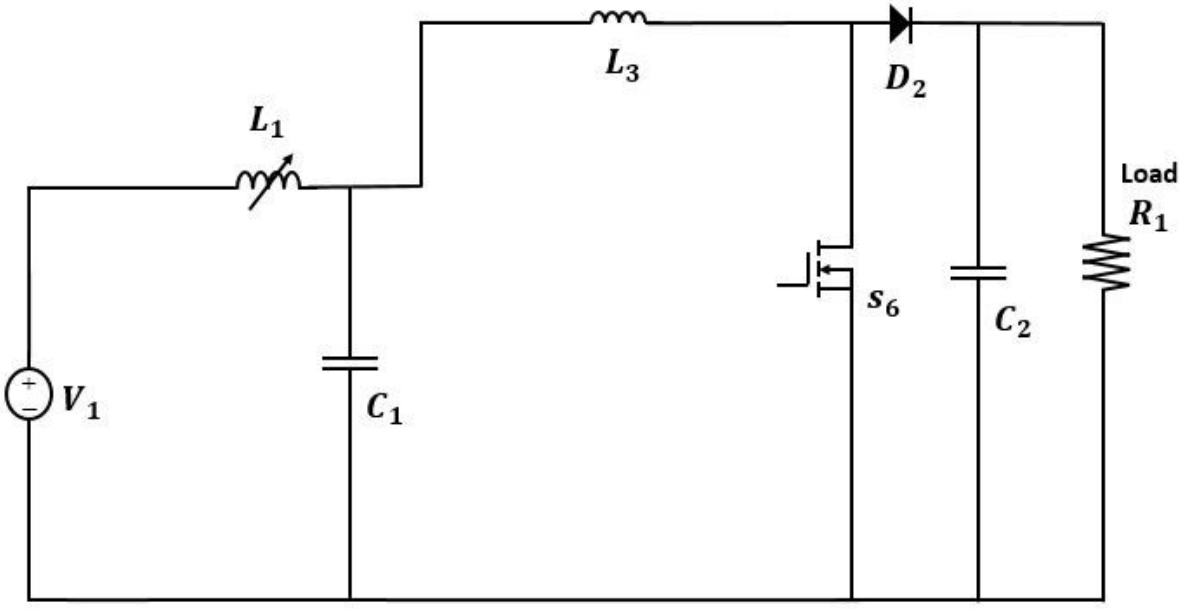

Fig 3.7: Mode III: Load supplying mode

Mode IV (S_5 & S_6 : on): In this mode the battery supplies energy to inductor L_3 and the load as the first source cannot supply enough energy ($V_1 < V_{\min}$). As the first source V_1 is below the required minimum voltage value, the battery is acting as the main supplier for the load through the boost stage as shown in Figure 3.8.

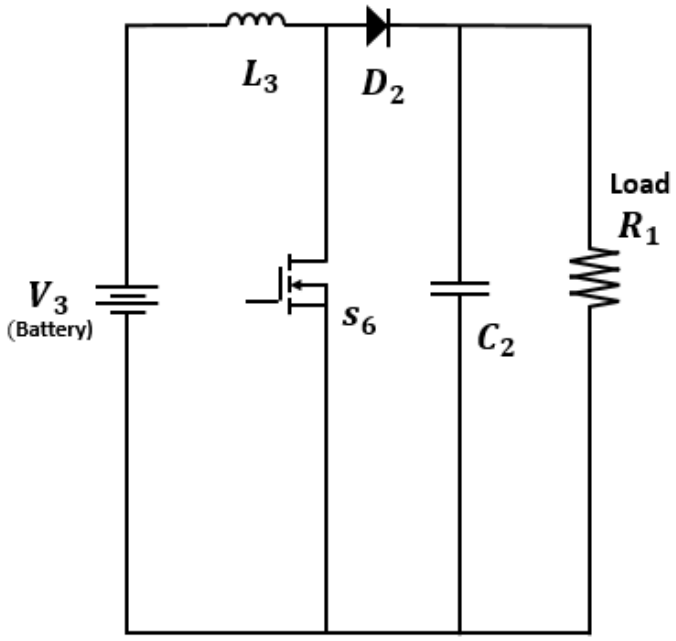

Fig 3.8: Mode IV: Load supplying and battery discharging mode

3.3. Control Structure

This section introduces the control system for the four operation modes of the converter. Figure 3.9 shows the control part of the topology were voltage and current sensors are used with the Proportional-Integral (PI) controllers and the control algorithm to switch between modes and to obtain the desired output power.

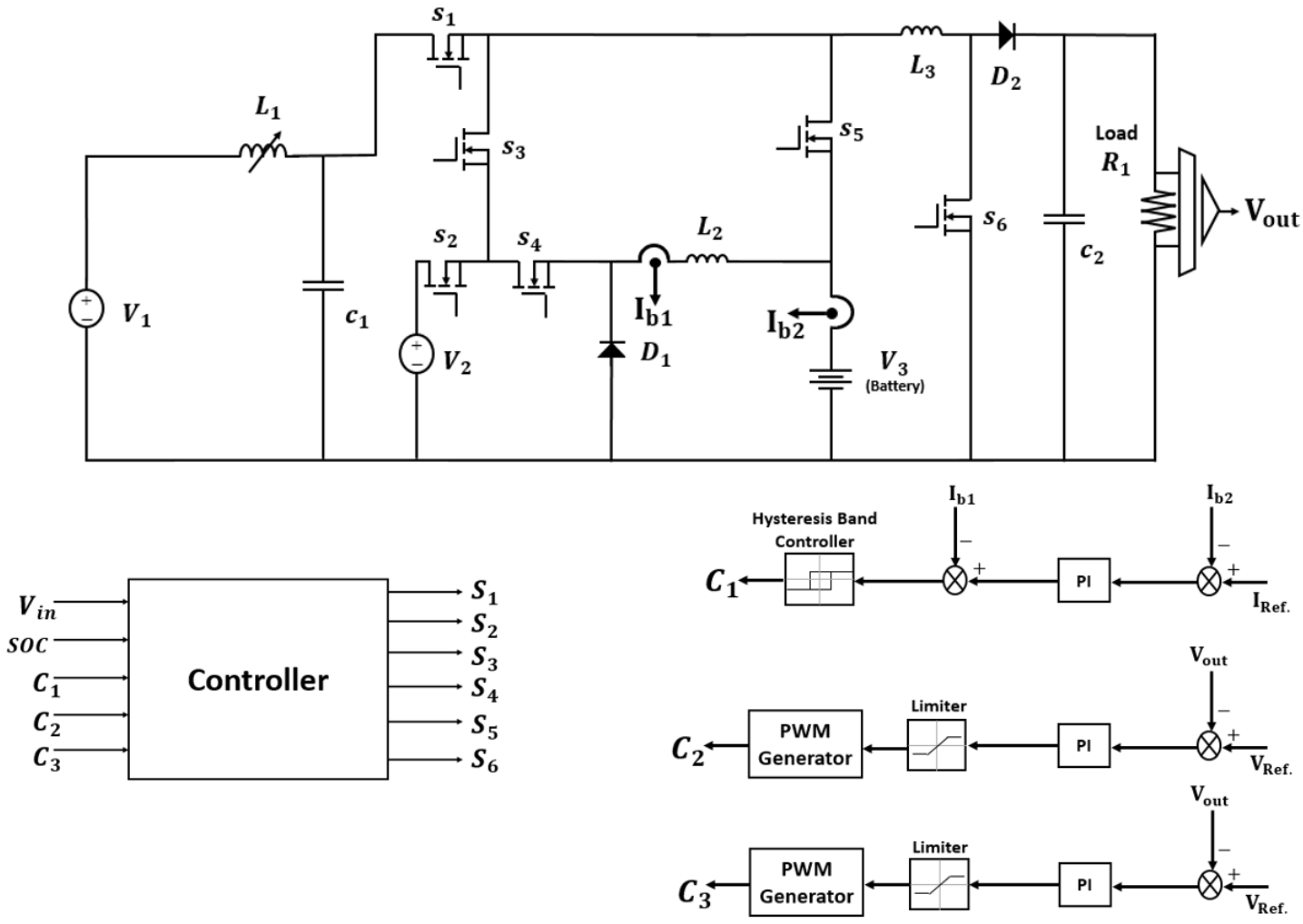

Fig 3.9: Control scheme

There are three PI controllers, two for voltage control and one for current control. The first one is used for buck stage for charging the battery using the two sources, the second one is used for boost stage for suppling the load using the first source and third one is used for boost stage for suppling the load using the battery. PI controller is selected as it is the most common control algorithm, it is easy, simple to implement and reliable for linear systems and it involves only two separate constants: the proportional and the integral.

PI controller is one of the PID controller categories which has three constants combined (Figure 3.10) and is used to control the steady-state and transient errors. The proportional constant determines the reaction to the current error, the integral constant determines the reaction based on the sum of recent errors and the derivative constant determines the reaction to the rate at which the error has been changing. Hence, the PID controller provides both an acceptable degree of error reduction and an acceptable stability and damping.

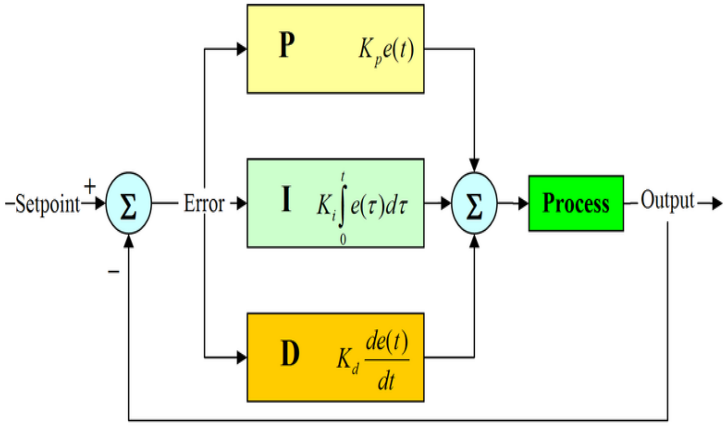

Fig 3.10: Block diagram of the PID controller

In order to get acceptable performance, the constants K_p, K_i and K_d can be adjusted, this adjustment process is called tuning the controller and by tuning the three constants, the controller can provide control action designed for specific process requirements.

The controller calculates an error value as the difference between a measured process variable and a desired set point and attempts to reduce the error by adjusting a manipulated variable (e) which is the tracking error, as shown in Figure 3.11, the error signal will be sent to the PID controller, and then the signal just past the

controller is now equal to the proportional gain times the magnitude of the error plus the integral gain times the integral of the error plus the derivative gain times the derivative of the error where, this signal will be sent to the plant, and the new output will be obtained.

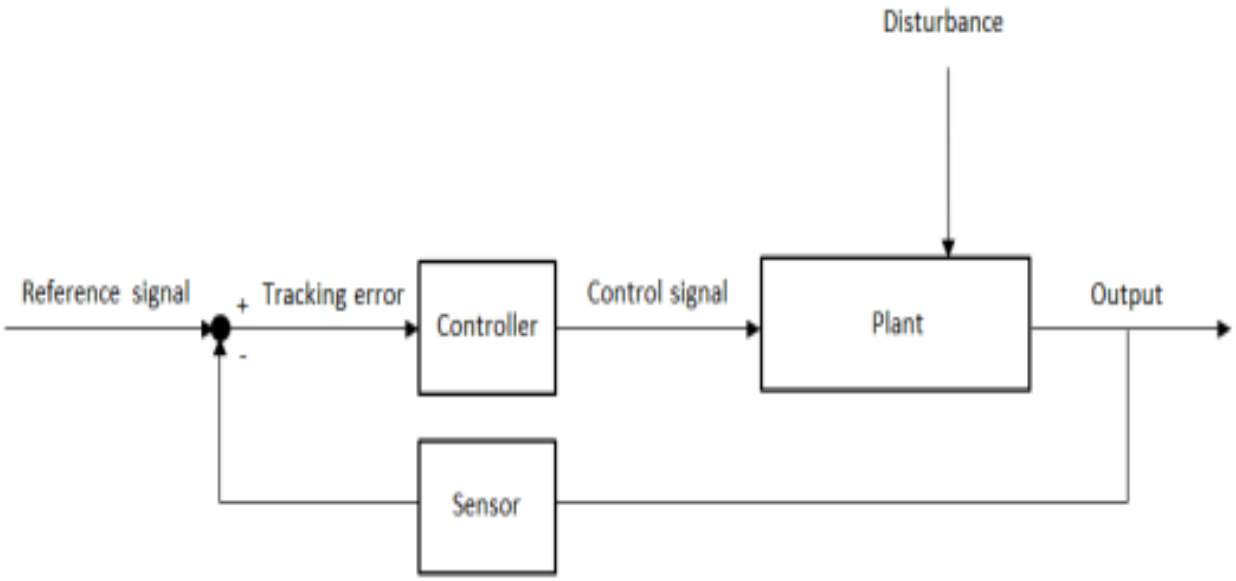

Fig 3.11: System block diagram with feedback control

Two different controllers are used, Proportional Integral (PI) controller and integral and Integral controller (I) which outputs a control signal that is proportional to the integral of the error signal.

The PI controller is used for the current and the voltage control for the boost stage when the battery is the supplier. The integral control is used for the voltage control for the boost stage when the first source is the supplier.

The difference between the two controllers is the transfer function of the system. For the Integral controller, the closed loop transfer function of the first order system is:

$$G(s) = \frac{\frac{K_I}{s}.K}{\tau\,.\,s + 1 + \frac{K_I}{s}.\,K} \tag{3.17}$$

Where τ is the time constant and K is the DC Gain.

Which leads to a plant transfer function of:

$$G_p(s) = \frac{1}{s+1} \tag{3.18}$$

The closed loop transfer function of the first order system of the PI controller is:

$$G(s) = \frac{\left(K_p + \frac{K_I}{s}\right).\,K}{\tau\,.\,s + 1 + \left(K_p + \frac{K_I}{s}\right).\,K} \tag{3.19}$$

Which leads to a plant transfer function of:

$$G_p(s) = \frac{1}{s^2 + s + 1} \tag{3.20}$$

So the implemented controller is shown in Figure 3.12 using the following equations according to the controller algorithm:

$$\frac{\mathrm{V_{out}(S)}}{\mathrm{V_{set}(s)}} = \frac{\mathrm{G(s)}}{1+\mathrm{G(s)}} \tag{3.21}$$

$$\mathrm{G(s)} = \mathrm{G_P(S).G_{PWM}(S).G_{DC-DC}(S)} \tag{3.22}$$

$$\mathrm{G_{conv}(s)} = \mathrm{G_{PWM}.G_{DC-DC}(S)} \tag{3.23}$$

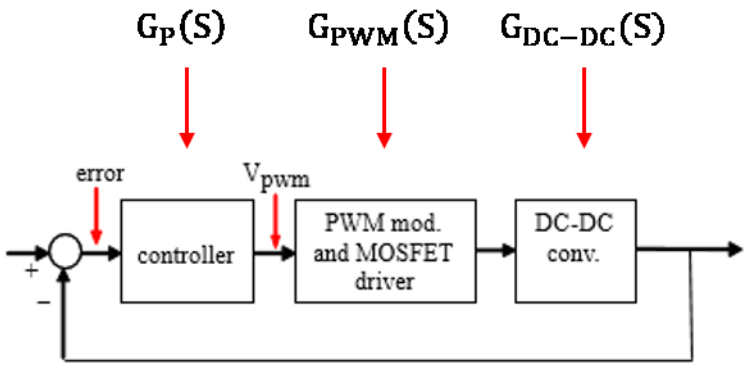

Fig 3.12: DC-DC Converter Process with Closed-Loop Controller

The frequency response and Bode plots of the two voltage controllers are shown in Figure 3.13 and 3.14 respectively as the controllers tune the signal according to the voltage variation to get the desired output.

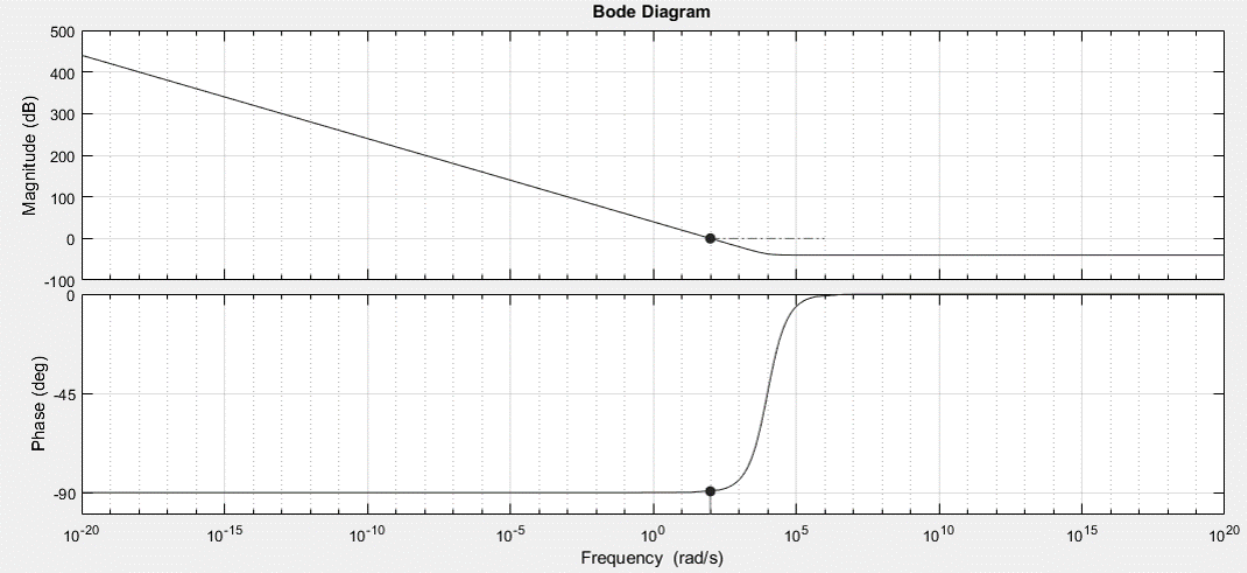

Fig 3.13: Voltage control for boost stage using the first source

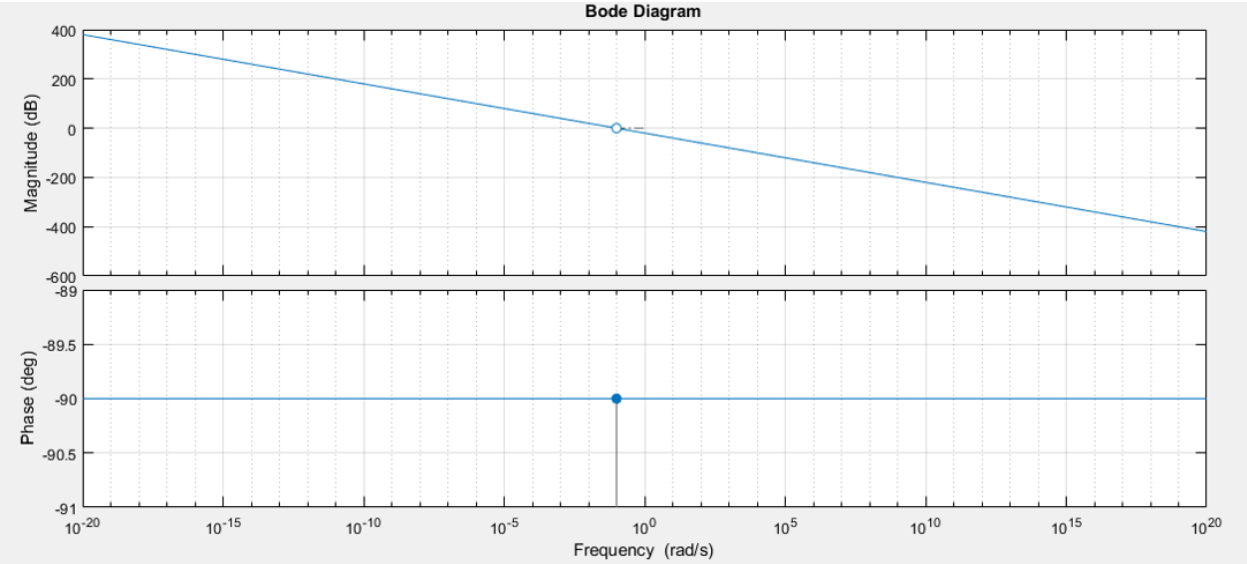

Fig 3.14: Voltage control for boost stage using the battery

The frequency response and Bode plot of the current controller is shown in Figure 3.15, as the controller tunes the signal according to the voltage variation to get the desired output.

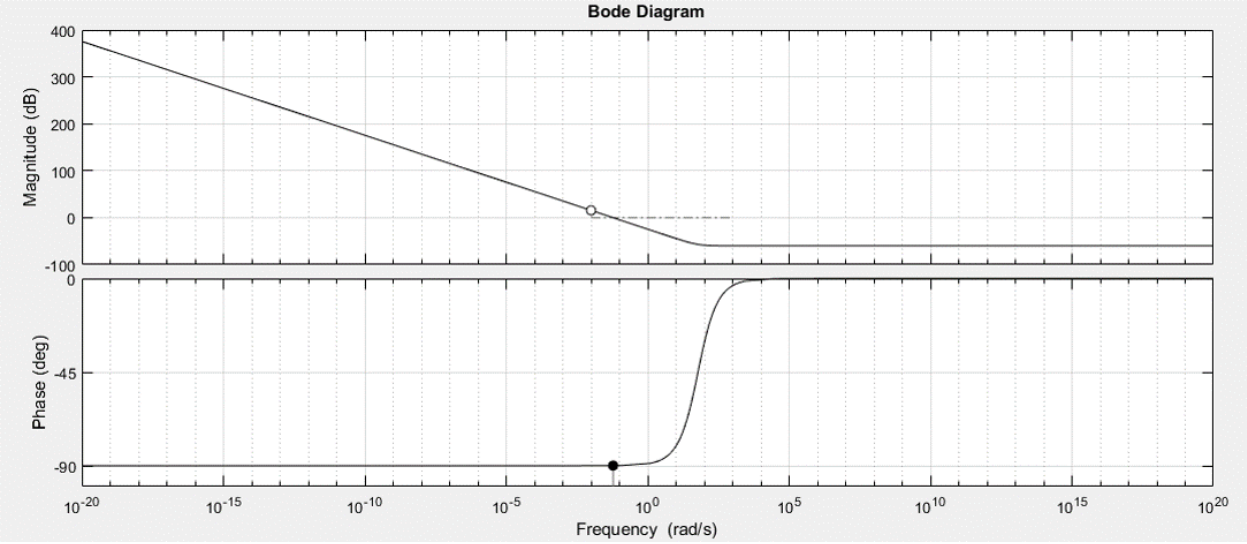

Fig 3.15: Current control for buck stage using one of the two sources

After getting the required signal from the PI controllers, the data is implemented into a unique control algorithm with the minimum value of the input sources and the maximum and minimum value of SOC for battery to switch between the operating modes. The control algorithm consists of two phases, Phase 1 analyze the input data and Phase 2 determine the suitable operation mode.

In Phase 1 (Figure 3.16), the control algorithm takes on the current values of the two input sources, the SOC of the battery and the output signals from the PI controllers as input data and then starts a comparison between them and the minimum values of the input sources and the minimum and maximum values of the SOC of the battery to implement an output data that will be used in the second phase.

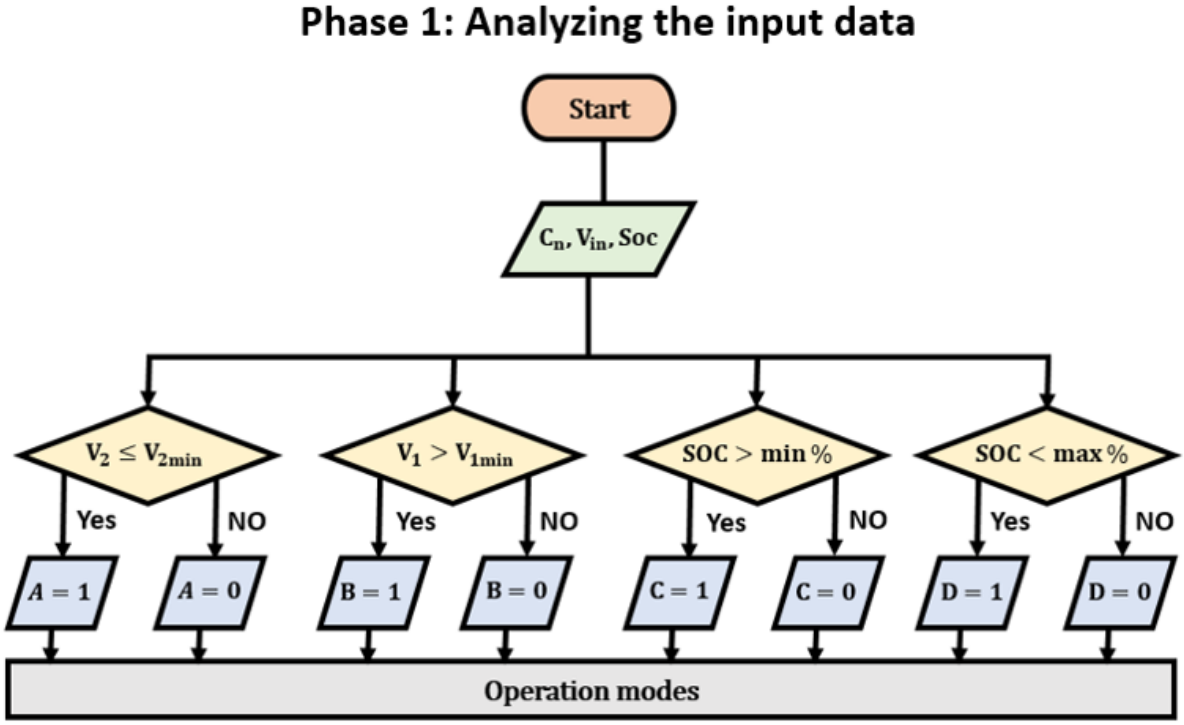

Fig 3.16: Control algorithm flow chart (1)

In Phase 2 (Figure 3.17), the output data is used to obtain 4 different scenarios to select the most suitable operation mode according to the current state of the input sources values and the SOC of the battery and when the data changes, it switches to another mode to ensure an effective energy management of the sources.

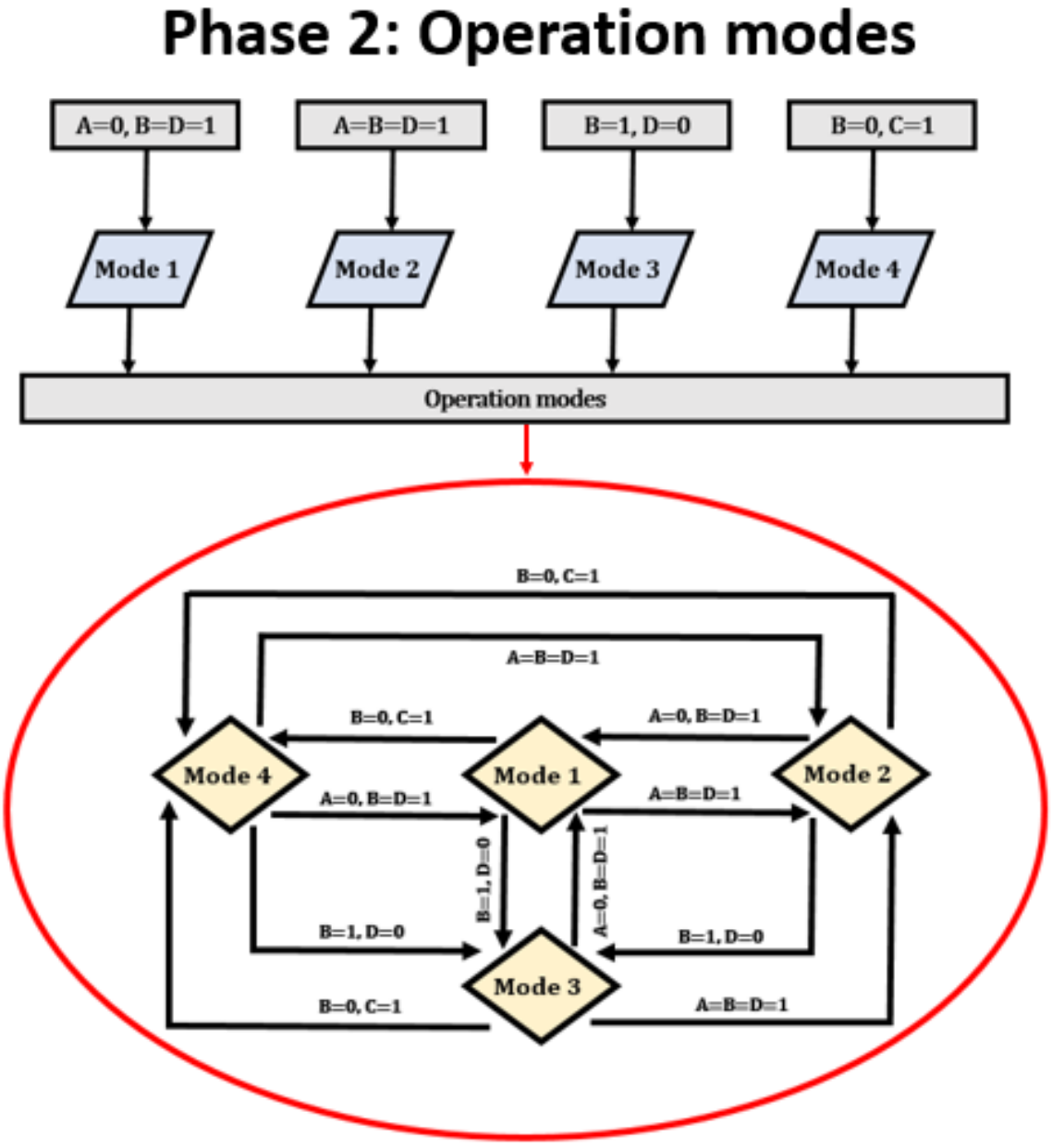

Fig 3.17: Control algorithm flow chart (2)

3.4. Applications

The converter was designed for DC microgrid applications and to utilize the PV energy sources as input sources for the system. The converter is also capable of utilizing different types of renewable energy sources by considering the characteristics of each source and the need of implementing an AC-DC converter if necessary. The converter can be used also for different types of DC load applications according to the required output power needed. The converter is suitable for 100 W to 100 kW power systems and the input sources and the battery specifications can be selected according to the desired application as shown in Figure 3.18.

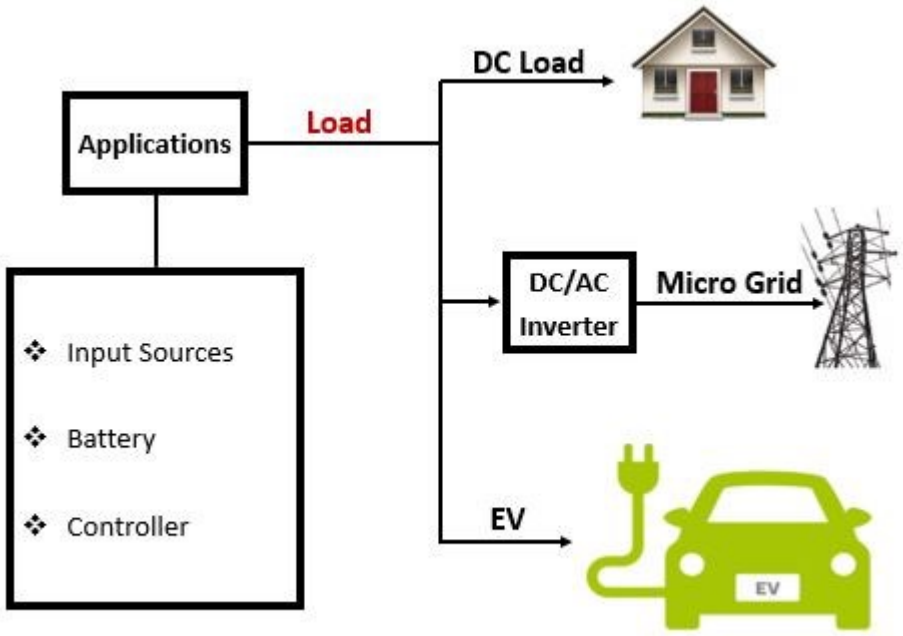

Fig. 3.18: Converter applications

Chapter 4
PV Systems

4.1. General

Renewable energy is produced from the sources that do not deplete or replenished within the human's life time and most of the energy sources are derived from the sun by capturing the sunlight directly using solar technologies. They are considered as the future of the supply systems as the energy demand is increasing and they are the solution to a lot critical concerns such as global warming and air pollution and reduction of fossil fuels. Renewable energy has unique benefits than the conventional as it is clean source of energy, can help developing countries from over reliance on fossil fuels, reliable source of energy as it depend on weather disruptions and they can continue to operate if one of the equipment in the system is damaged, low to zero maintenance required, stable energy prices, economical benefits and improving public health. They are commonly used because of the energy dependence, low carbon technologies and sustainability but there are a lot concerns related the best utilization method of renewable sources such as voltage regulation, network stability and power quality.

4.2. PV Generation

Photovoltaic (PV) systems [20] use solar cells to convert sunlight into electricity and the amount of electric power generated changes continuously with weather conditions. The solar cells working principle is based on the photovoltaic effect and generation of a potential difference at the junction of two different

materials in response to electromagnetic radiation. The photovoltaic effect is similar to the photoelectric effect, where electrons are emitted from a material that has absorbed light with a frequency above a material dependent threshold frequency.
The PV generation consists of an arrays of solar or photovoltaic cells for the energy conversion as shown in Figure 4.1 and the advantages includes longer life, easy installation, environmental friendliness and energy dependence.

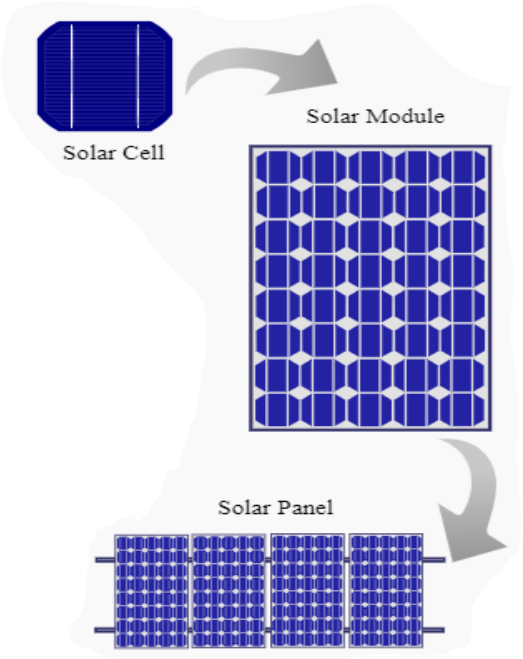

Fig 4.1: PV arrays

The photovoltaic system [21] depends on the solar module and it consists of many photovoltaic cells which are wired together by the manufacturer. The solar modules are wired together in series to form strings and strings of modules are connected in parallel to form an array. The photovoltaic system can be selected according to the rated power which is the maximum power the panel can produce with 1000 watts of sunlight at module temperature of 25 Celsius and the system voltage which usually provides from 235 volt to 600 volt without using batteries. It is very important to select the required module for system as module costs and efficiencies continue to

change as technology and manufacturing methods improve, so module comparisons are made according to the current information and the specific requirements of the desired application. The selection of the module will depend on the rated power, module cost per watt as the thin film modules have lower costs than crystalline silicon modules and the module efficiency as higher efficiency required a smaller area to achieve the same output power of an array so the installation and racking costs will be less.

The PV system can operates at maximum efficiency and produces maximum output power by implementing a maximum power point tracking (MPPT) algorithm [22] which is a specific point on the V-I curve of the PV array, so by tracking the MPPT the system will be able to extract the maximum power available from a PV module under different conditions.

4.3. Modeling of the PV Module

The simplest equivalent circuit of a solar cell is a current source in parallel with a diode as shown in Figure 4.2 .The output of the current source is directly proportional to the light absorbed by the cell and during darkness, it generates diode current and the diode determines the I-V characteristics of the cell.

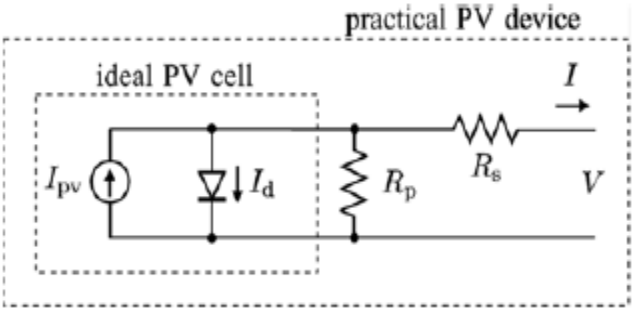

Fig 4.2: Circuit diagram of the PV model

An existing modeling of the PV module [23] can be used in the simulation process to validate the utilization of PV sources with the converter topology and to apply variable input voltage to the converter by using different Irradiance and temperature values as shown in Figure 4.3. The first step is choosing a PV module, knowing the number of cells per module and arrays required in series or parallel for the desired power, voltage and current. The second step is using numerical methods and the same model parameters and equations to calculate the all of the necessary parameters for obtaining the variables Voltage (V), Irradiation (G), and Temperature (T).

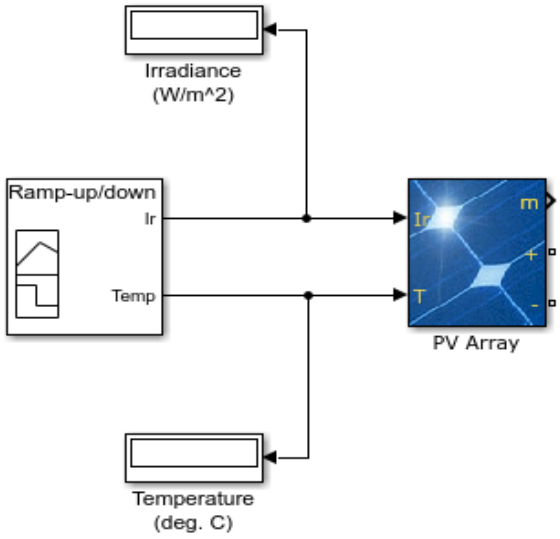

Fig 4.3: PV system

The following equations can be used for this modelling, which include temperature dependence of the photocurrent I_{PV} and the saturation current of the diode I_O, starting with the net current of the cell which is the difference of the photocurrent, I_{PV} and the normal diode current I_O:

$$I = I_{pv} - I_0[e^{\frac{q(v+IR_S)}{nKT}} - 1] \qquad (4.1)$$

$$I_{pv} = I_{pv}(T_1) + K_0(T - T_1) \qquad (4.2)$$

The proportionality constant in (4.3) is set so the rated short circuit current is delivered under rated irradiation:

$$I_{pv}(T_1) = I_{sc}(T_1)\frac{G}{G(nom)} \qquad (4.3)$$

The change of photo current with the change of temperature in (4.4.4) is used to deduce the relationship between the photo current and temperature in (4.4.2) which is linear:

$$K_0 = \frac{I_{sc}(T_2) - I_{sc}(T_1)}{T_2 - T_1} \qquad (4.4)$$

$$I_0 = I_0(T_1) \times \left(\frac{T}{T_1}\right)^{\frac{3}{n}} . e^{\frac{q.v_{g(T_1)}}{nK(\frac{1}{T} - \frac{1}{T_1})}} \qquad (4.5)$$

The value of the saturation current is calculated using the open circuit voltage and short circuit current at reference cell operating temperature:

$$I_0(T_1) = \frac{I_{sc}(T_1)}{(e^{\frac{q.v_{OC}(T_1)}{nKT_1}} - 1)} \qquad (4.6)$$

Series resistance Rs represents the resistance inside each cell in the connection between cells:

$$R_s = -\left(\frac{d_v}{d_I}\right)|v_{oc} - \left(\frac{1}{X_v}\right) \quad (4.7)$$

$$X_v = I_0(T_1)\frac{q}{nKT_1}.e^{\frac{q.v_{oc}(T_1)}{nKT_1}} \quad (4.8)$$

All of the constants are provided by the manufacturer's ratings of the PV array and the parameters for the equations are listed in Table 4.1.

Table 4.1: Parameters Symbol definition

q	Electron charge($1.60217646 \times 10^{-19}$C)
K	Boltzmann constant ($1.3806503 \times 10^{-23}\ ^{J}/_{K}$)
V	Cell output voltage (V)
V_g	Band gab voltage (V)
n	Diode quality factor
T_1	Reference cell operating temperature (25 C)
T_2	Another Cell operating temperature (75 C)
I_{sc}	Short circuit current at the standard condition (A)
V_{oc}	Open circuit voltage at the standard condition (V)
N_{ser}	No. of series connected modules per string
N_{par}	No. of parallel strings

Chapter 5
Results

This chapter discusses the results obtained from the modeling of the proposed topology using Matlab Simulink software to show the behavior of the converter with the considerations of varying input voltages. It also discusses the results obtained from the prototype hardware implementation to test the converter effectiveness.

5.1. Simulation Results

All modes of operation were tested with a 300W system to obtain a fixed output power using two input sources and a battery. The switching commands have a variable duty ratio at a switching frequency of 30 kHz. Simulation results were obtained to validate the proposed topology. The results of each mode of operation, behavior of the battery during the charging/discharging process, and showing the duty ratio according to different input voltage values are provided and The parameters used for this simulation are given.

5.1.1. Design parameters

The maximum value for the two input sources and the battery specifications were selected to obtain 300W system. The other parameters were calculated according to the boost and buck stages. The important parameters are listed in Table 5.1.

Table 5.1: Simulation design parameter

Parameter	Value
V1	50 V
V2	50 V
Load R1	33.33 Ω
Switching frequency (fs)	30 kHz
L2	555 µH
L3	1.388 mH
C2	10 µF
V3 (Battery)	15 V

5.2. Experimental Results

A DC power supply, load simulator and dSPACE controller are used in the protoype to confirm the simulation results and topology concept. The power supply is 12 kW multi power supply to implement two input sources and the electronic load simulator was used to verify the converter efficiency with different loads and an external two load resistors were used for validation. Switches and silicon isolated gate drivers were used for the control process and to change between different modes with the use of external AC-DC power supply.

The dSPACE was used to control the pulse width modulation (PWM) and switching process according to control algorithm. For the hardware implementation of the converter, two different sources were used, each is 50 V and for the first three modes, a 12.5 V battery was used while a 25 V battery was used for last mode. The results

of each mode was analyzed to get the input power, out power and efficiency of each stage.

The power stage's input port, battery port and output port are marked as shown in Figure 5.1. It consists of three boards, all feedback control loops compensators are implemented by dSPACE through soft switching and an external power supply is used to power up the gate drivers. A multi-input power supply of 12 kW was used to act as DC sources to replace the PV sources and to vary the input voltage to get the performance of the converter in each mode.

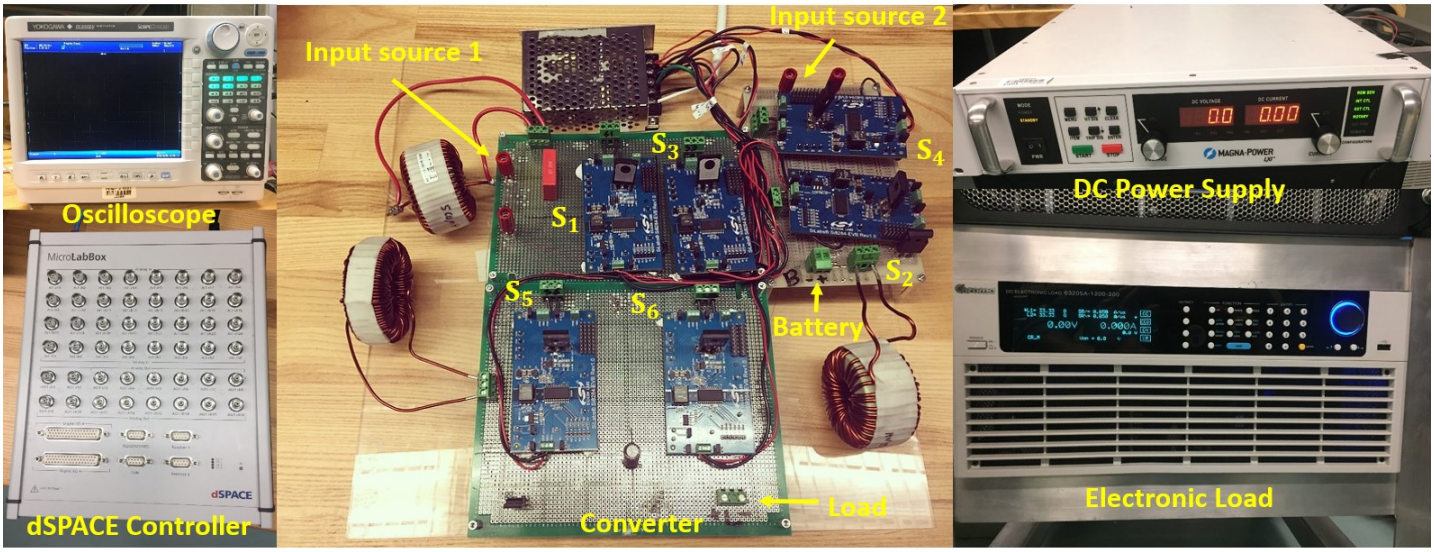

Fig 5.1: Hardware prototype

5.2.1. Design parameters and components

All of the components and parameters listed in Table 5.2 and Table 5.3 are selected to compare the performance of the converter between the simulation and experimental results. The specifications of the MOSFETS, diodes and gate drivers

listed in Table 5.3 are selected according to the maximum and minimum voltage and current levels in each of the operation modes.

Table 5.2: Hardware parameters

Parameter	Value	No.
Inductor (L1)	555 μH	1
Inductor (L2)	555 μH	1
Inductor (L3)	1.388 mH	1
Capacitor (C1)	0.6366 μF	1
Capacitor (C2)	10 μF	1
Resistance (R1)	28 Ω	1

Table 5.3: Hardware Components

Component	Specifications	No.
MOSFET	IPW65R070C6	6
Diode	IDV20E65D1	2
Gate Drivers	Si8284-EVB	6

All of the components were tested for a conventional boost-buck operations first with the same input and output powers to ensure that they will be suitable to use for the proposed converter. Gate drivers are selected according to the components values and specifications to control the switches and to change the operation modes according to the control system algorithm.

5.3. Results of Each Mode

1) Load supplying and battery charging (Vin1 & Vin2):

Two sources were used to supply the load and to charge the battery at the same time, fixed output was obtained through the output voltage and current, achieving 300W as required. Figure 5.2 shows the simulation results of the output behavior of the load during the boost stage. A DC voltage source V_1= 45 V is used.

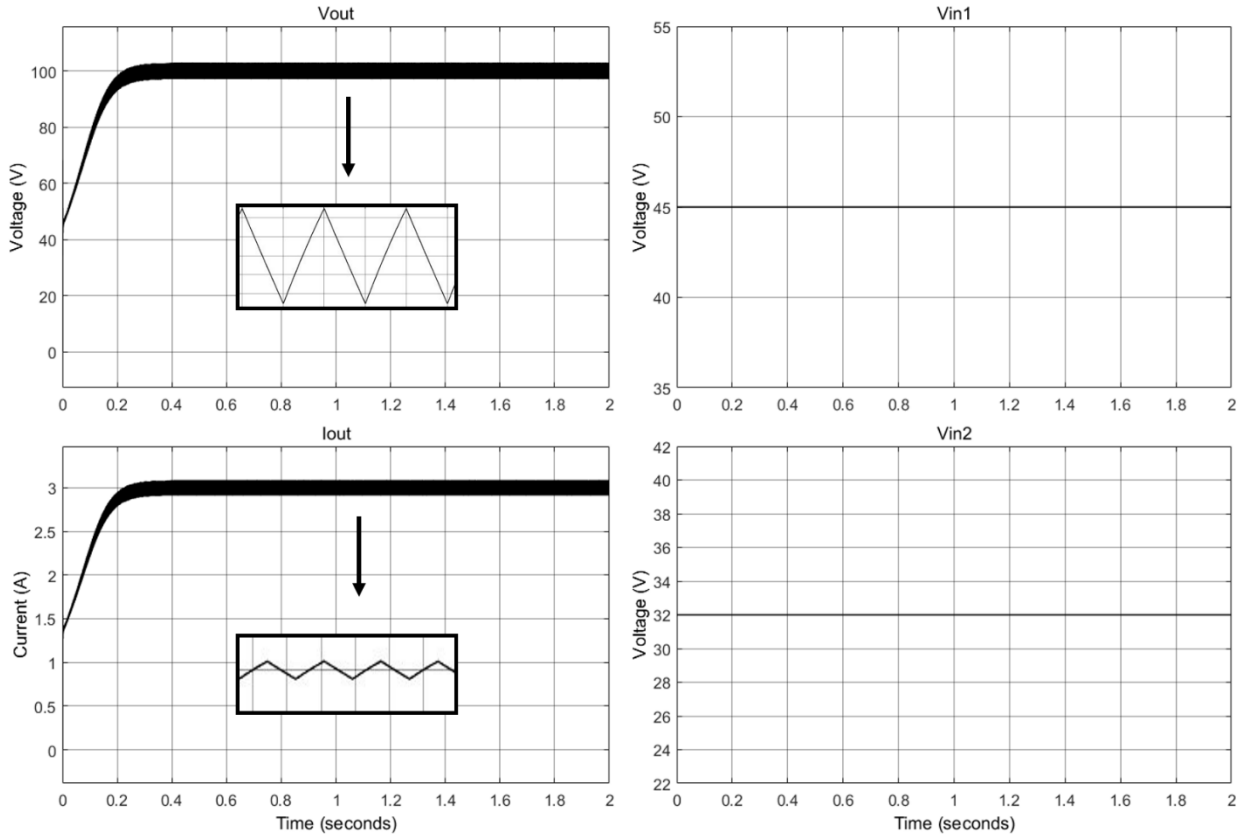

Fig 5.2: Simulation results during the first mode (load)

Figure 5.3 shows the experimental results of the output behavior of the load during the boost stage, and it is typical of the simulation results of the first mode. A DC voltage source V_{in}=50V is used. From top to bottom are the waveforms of output voltage V_o, output current I_o and switching commands S_6 and S_1. The switching commands S_6 and S_1 have duty ratios of 0.5 and 1 at switching frequency of 30 kHz respectively.

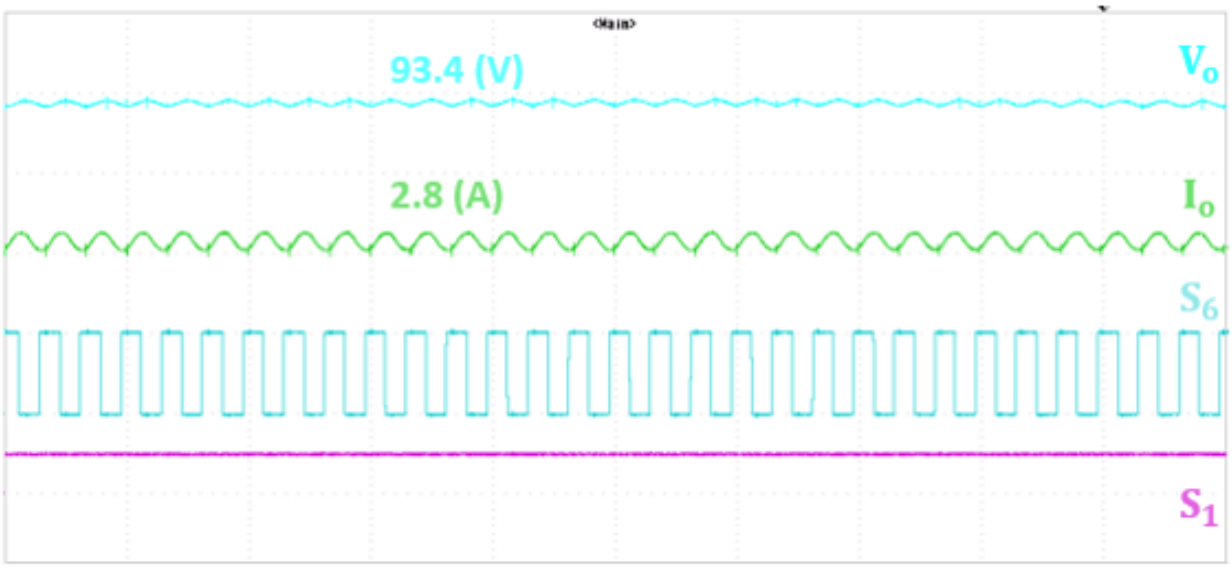

Fig. 5.3: Output behavior for Boost stage in Mode I

Figure 5.4 shows the dynamic response of the converter for the first mode with the output behavior of the load and how the controller tune the signal with a fixed settling time (84 ms) according to the variation of the input voltage level:

1) $V_1 = 50$ V

2) $V_1 = 37$ V

3) $V_1 = 25$ V

4) $V_1 = 43$ V

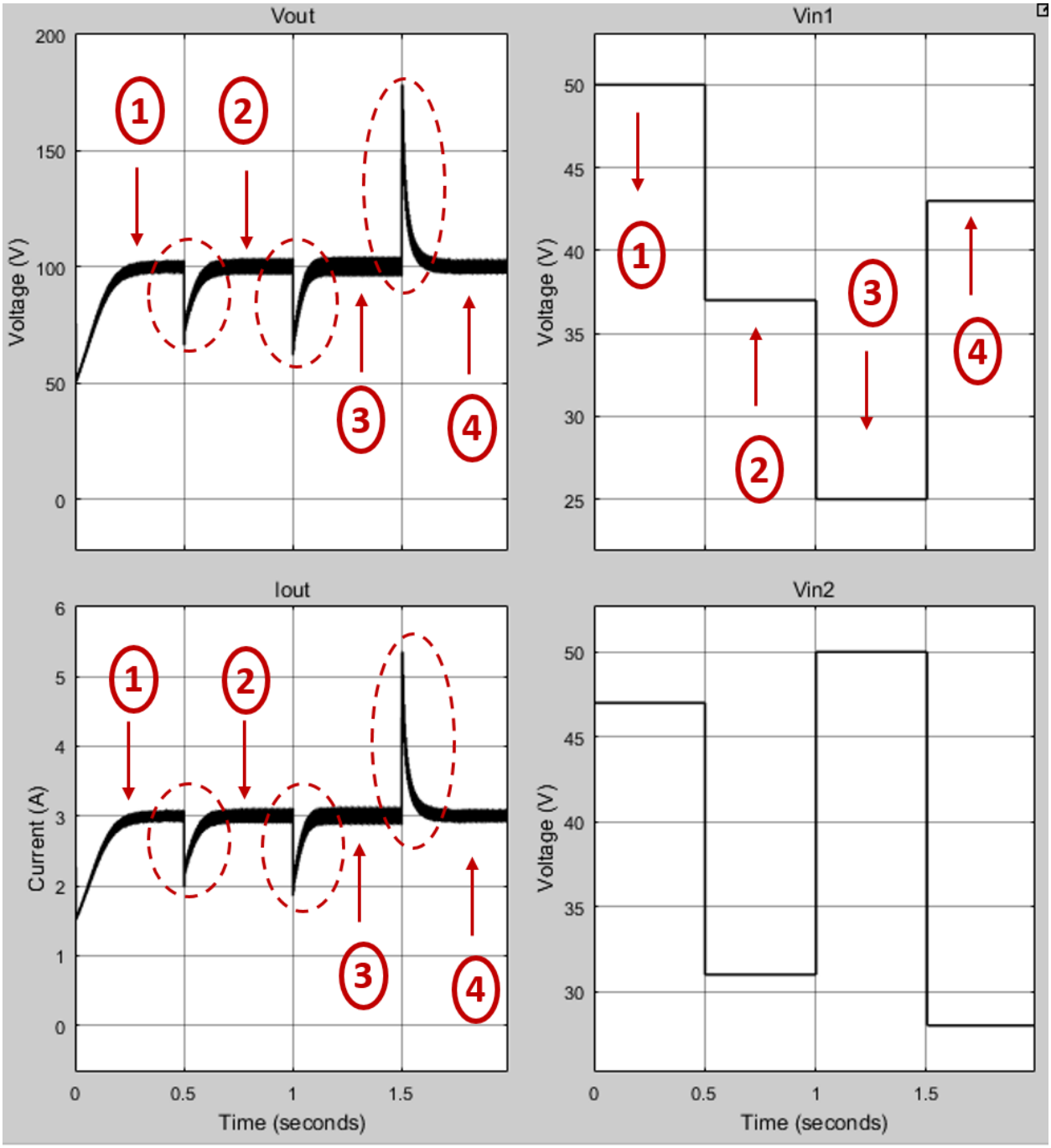

Fig 5.4: Dynamic response during the first mode (load)

Figure 5.5 shows the simulation results of the output behavior of the battery during the charging process in the buck stage. A DC voltage source V_2= 32 V is used.

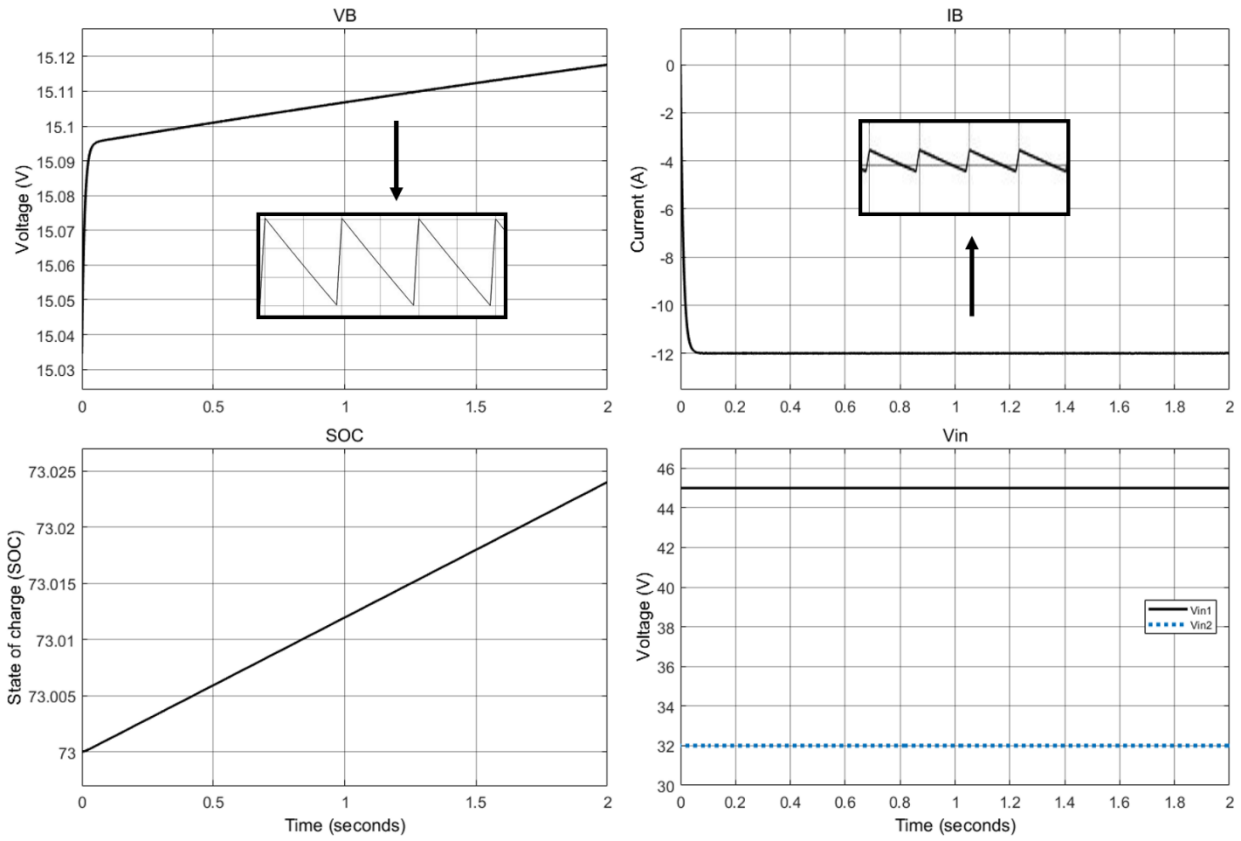

Fig 5.5: Simulation results during the first mode (battery)

Figure 5.6 shows the experimental results of the output behavior of the battery during the buck stage, and it is typical of the simulation results of the first mode. A DC voltage source V_{in}=50V and a 12.5 V battery are used. From top to bottom are the waveforms of output voltage V_o, output current I_o and switching commands S_2 and S_4. The switching commands S_2 and S_4 have duty ratios of 1 and 0.25 at switching frequency of 30 kHz respectively.

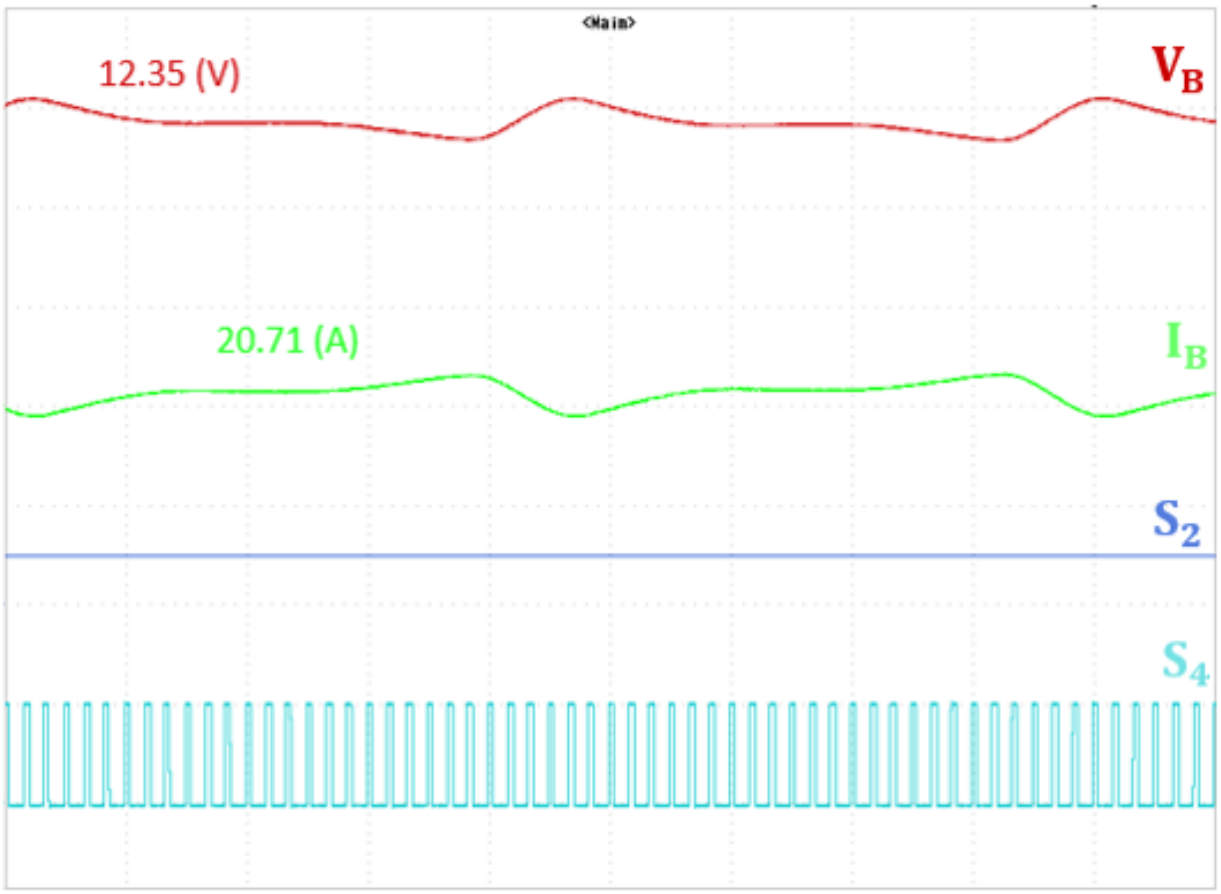

Fig 5.6: Output behavior for Buck stage in Mode I

Figure 5.7 shows the dynamic response of the converter for the first mode with the output behavior of the battery according to the variation of the input voltage level:

1) $V_2 = 47$ V

2) $V_2 = 31$ V

3) $V_2 = 50$ V

4) $V_2 = 28$ V

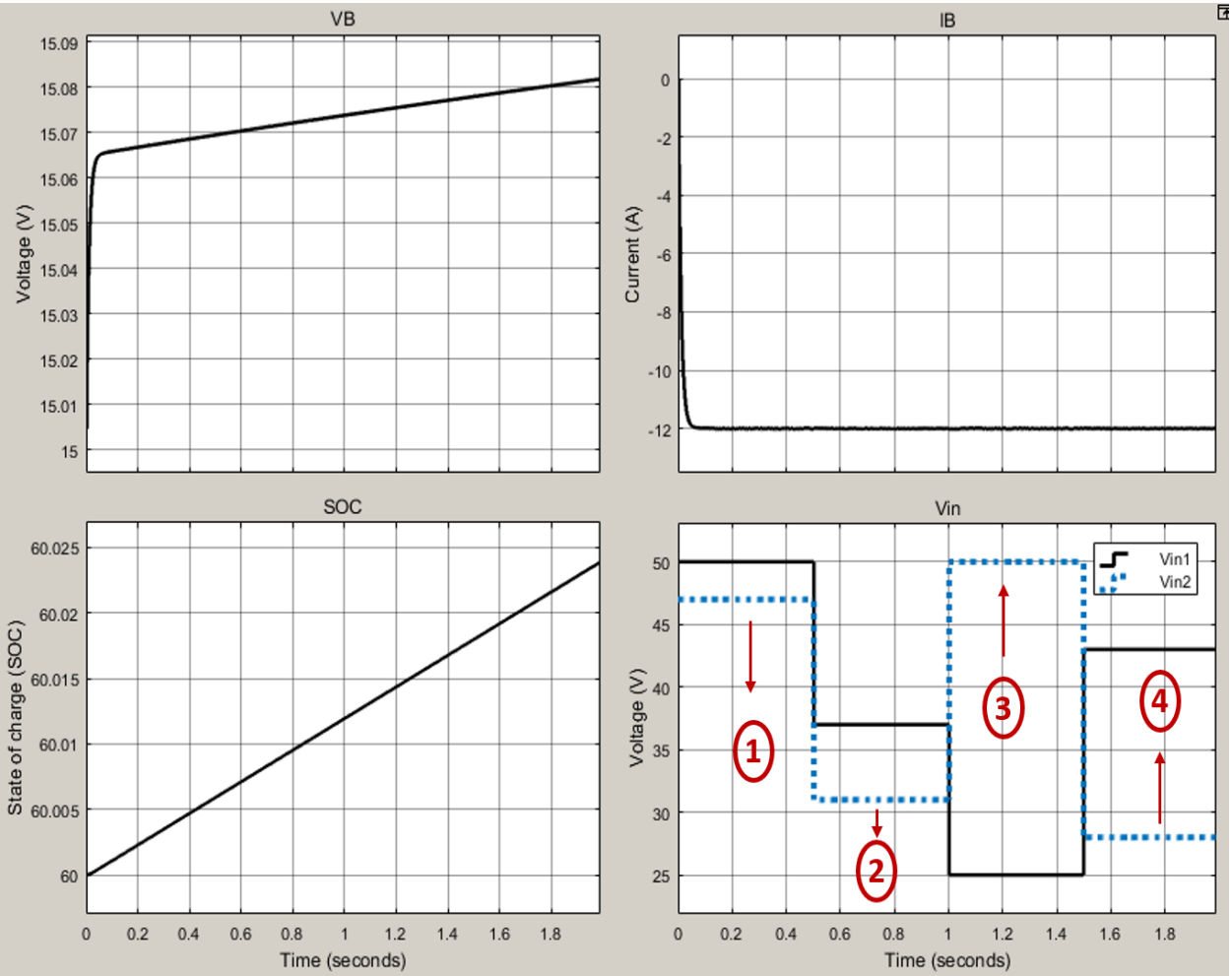

Fig 5.7: Dynamic response during the first mode (battery)

2) Load supplying and battery charging (Vin1):

One source was used to supply both load and battery at the same time as the other source failed to work. The mode works successfully in the boost and buck stages using one source, maintaining the same output power (300W). Figure 5.8 shows the simulation results of the output behavior of the load during the boost stage. A DC voltage source V_1= 50 V is used.

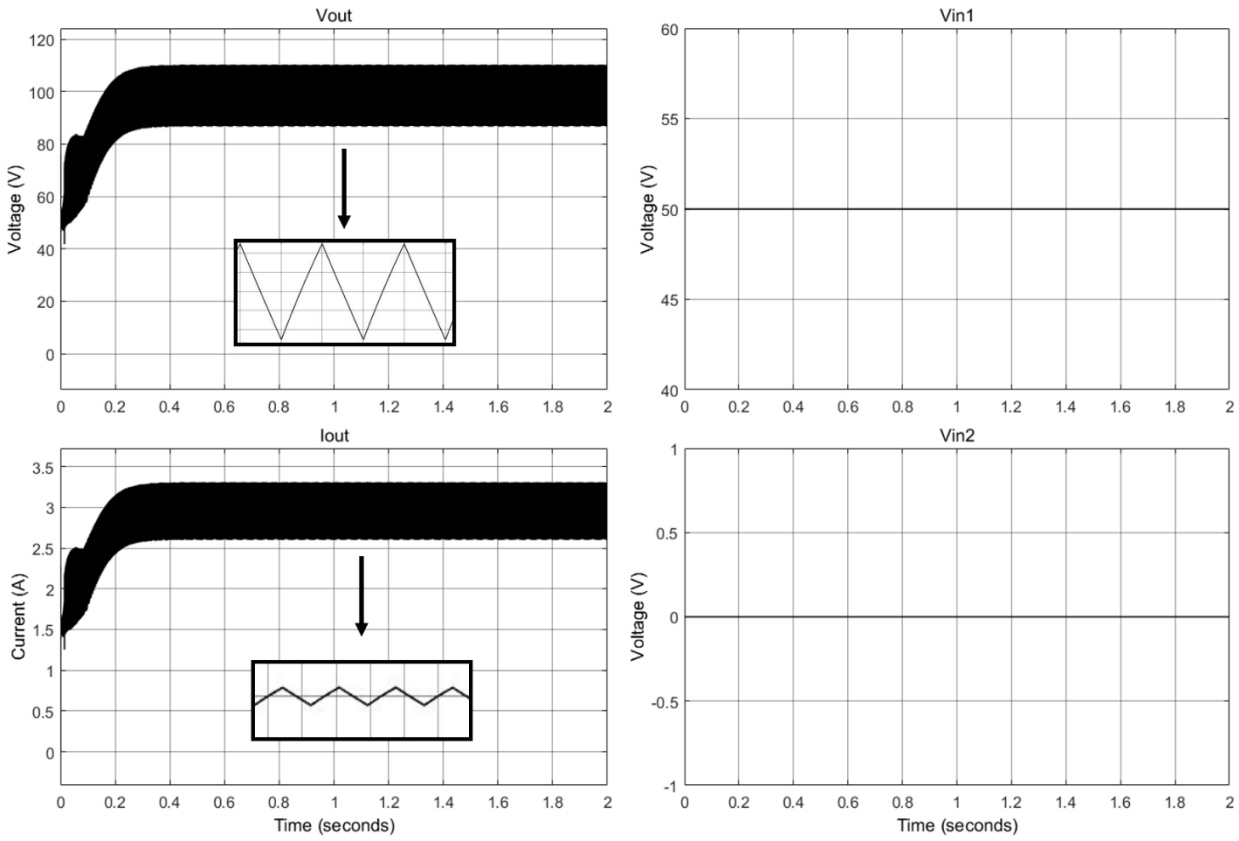

Fig 5.8: Simulation results during the second mode (load)

Figure 5.9 shows the experimental results of the output behavior of the load during the boost stage, and it is typical of the simulation results of the second mode. A DC voltage source V_{in}= 40 V is used. From top to bottom are the waveforms of output voltage V_o, output current I_o and switching commands S_6 and S_1. The switching commands S_6 and S_1 have duty ratios of 0.6 and 1 at switching frequency of 30 kHz respectively.

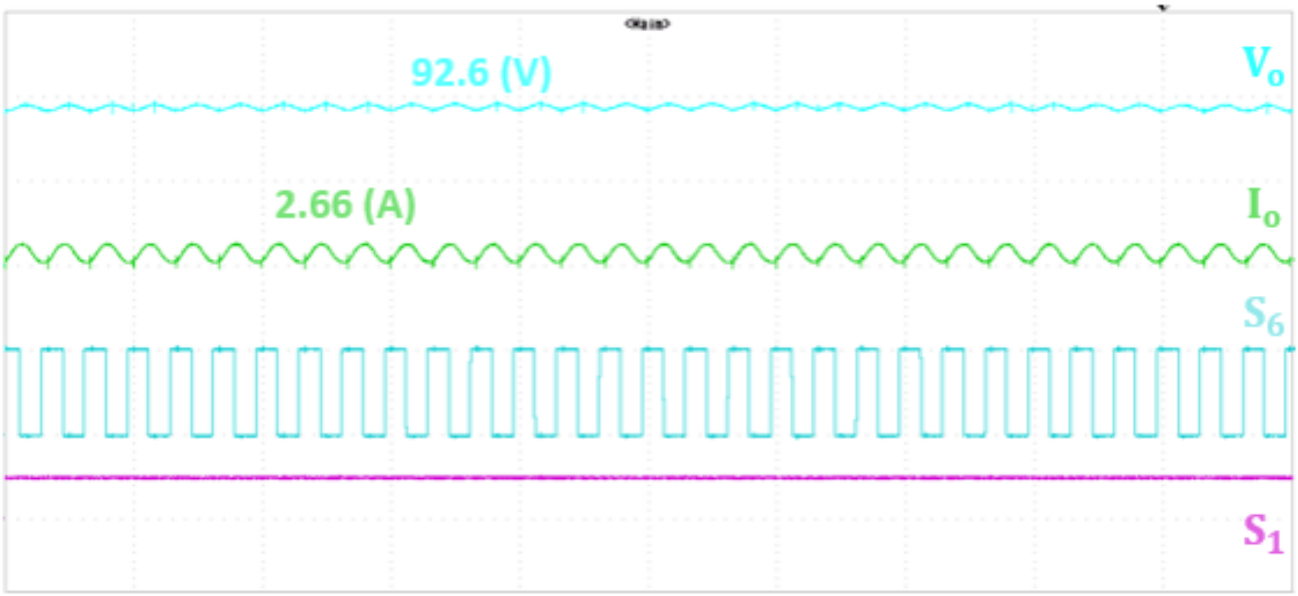

Fig 5.9: Output behavior for Boost stage in Mode II

Figure 5.10 shows the dynamic response of the converter for the second mode with the output behavior of the load and how the controller tune the signal with a fixed settling time (84 ms) according to the variation of the input voltage level:

1) $V_1 = 50$ V

2) $V_1 = 41$ V

3) $V_1 = 34$ V

4) $V_1 = 25$ V

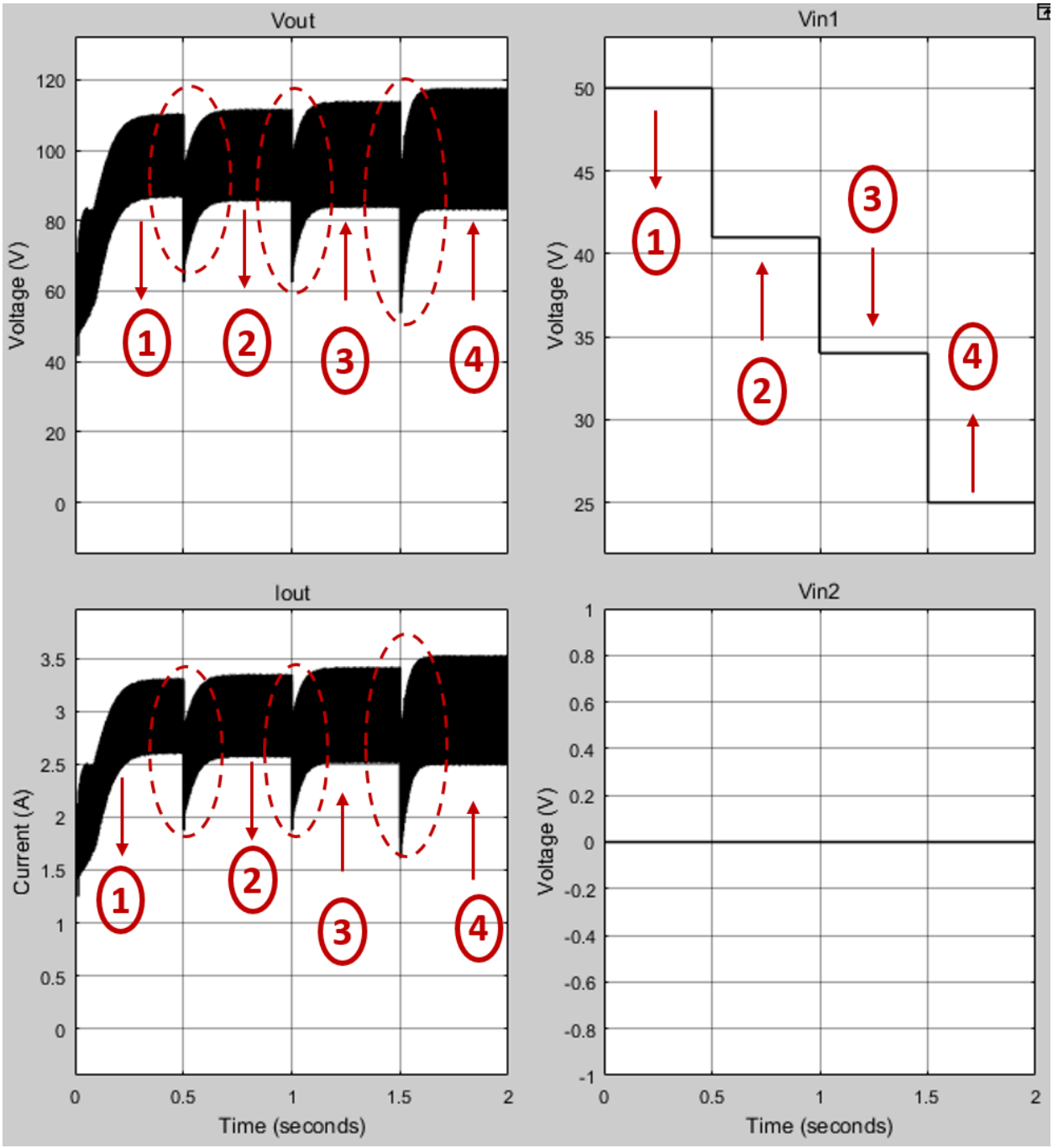

Fig 5.10: Dynamic response during the second mode (load)

Figure 5.11 shows the simulation results of the output behavior of the battery during the charging process in the buck stage. A DC voltage source V_1= 50 V is used.

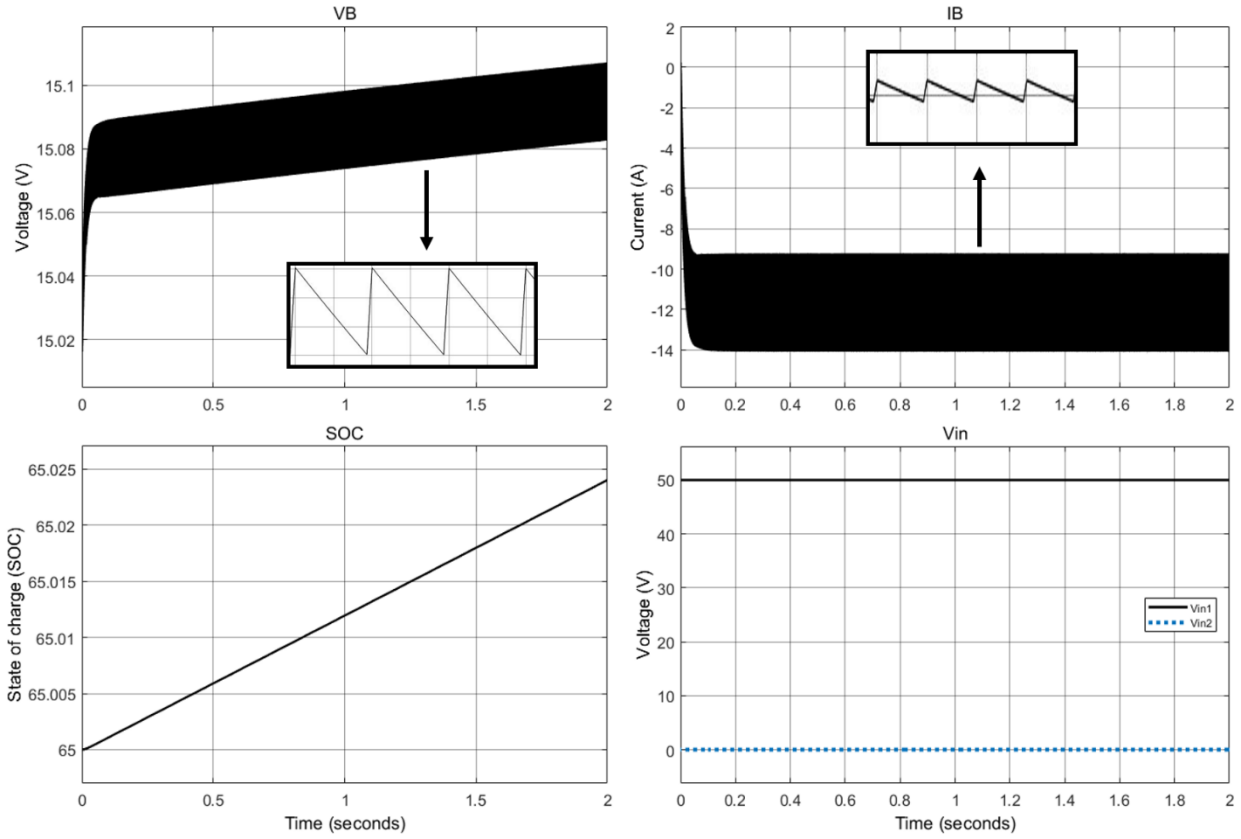

Fig 5.11: Simulation results during the second mode (battery)

Figure 5.12 shows the experimental results of the output behavior of the battery during the buck stage, and it is typical of the simulation results of the second mode. A DC voltage source V_{in}= 35V and a 12.5 V battery are used. From top to bottom are the waveforms of output voltage V_o, output current I_o and switching commands S_1, S_3 and S_4. The switching commands S_1, S_3 and S_4 have duty ratios of 1, 1 and 0.357 at switching frequency of 30 kHz respectively.

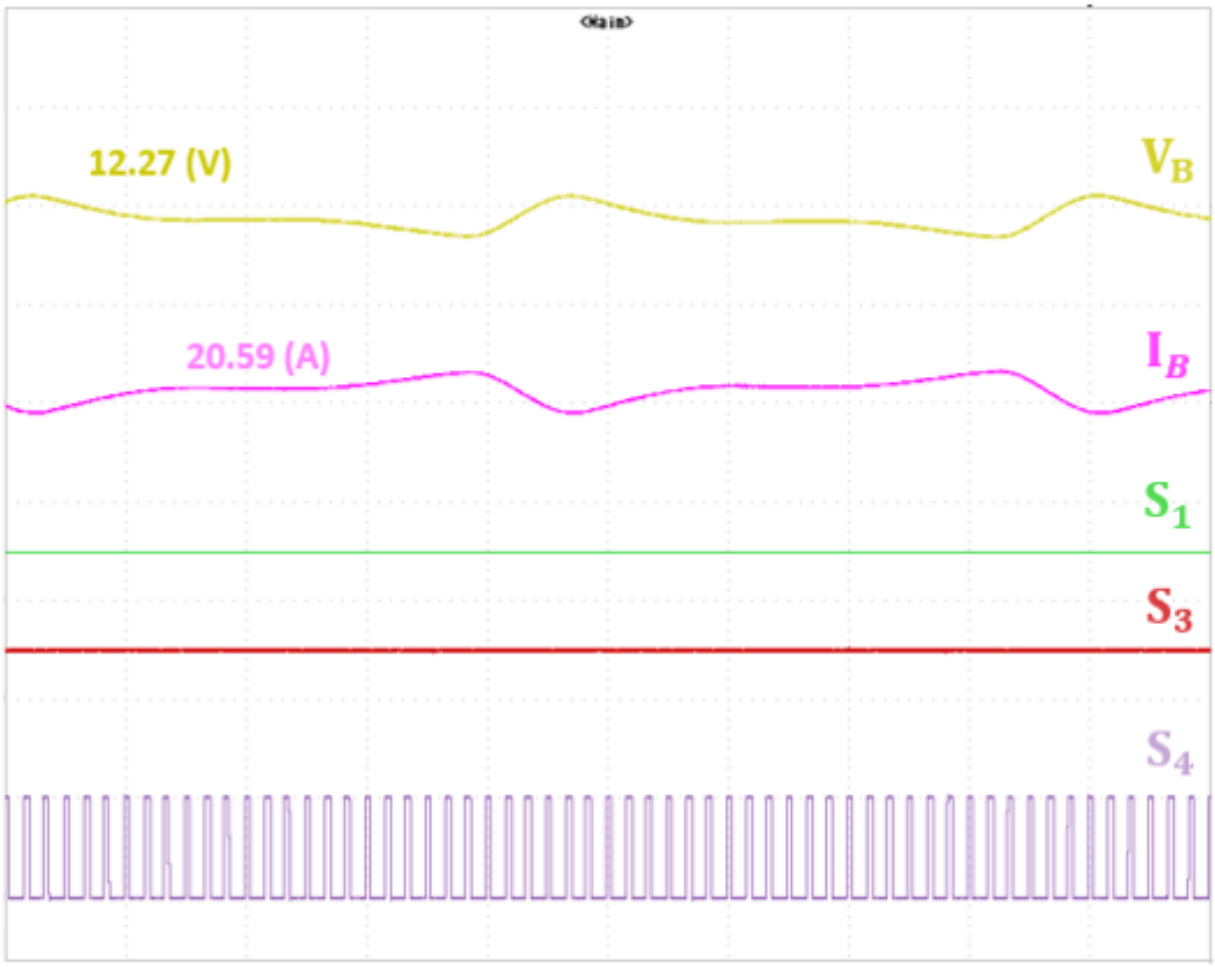

Fig 5.12: Output behavior for Buck stage in Mode II

Figure 5.13 shows the dynamic response of the converter for the second mode with the output behavior of the battery and how the controller tune the signal with a fixed settling time (84 ms) according to the variation of the input voltage level:

1) $V_1 = 50$ V

2) $V_1 = 41$ V

3) $V_1 = 34$ V

4) $V_1 = 25$ V

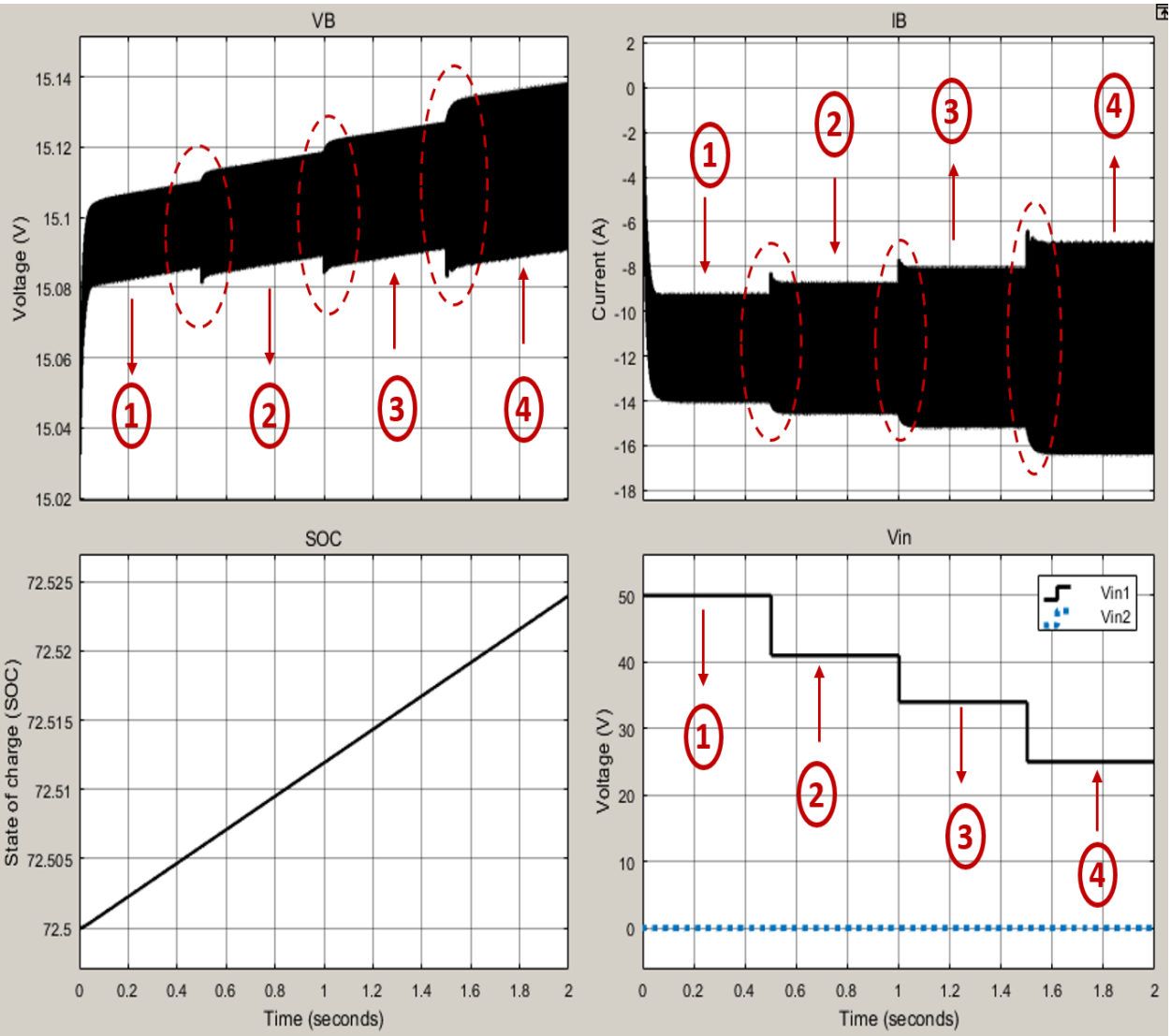

Fig 5.13: Dynamic response during the second mode (battery)

3) Load supplying (Vin1):

As the SOC of the battery reaches 90%, the first source V1 started to supply the load through the boost stage and cutting the second source from suppling the battery to increase the battery life time. Figure 5.14 shows the simulation results of the output behavior of the load during the boost stage. A DC voltage sources V_1= 50 V and V_2= 50 V are used.

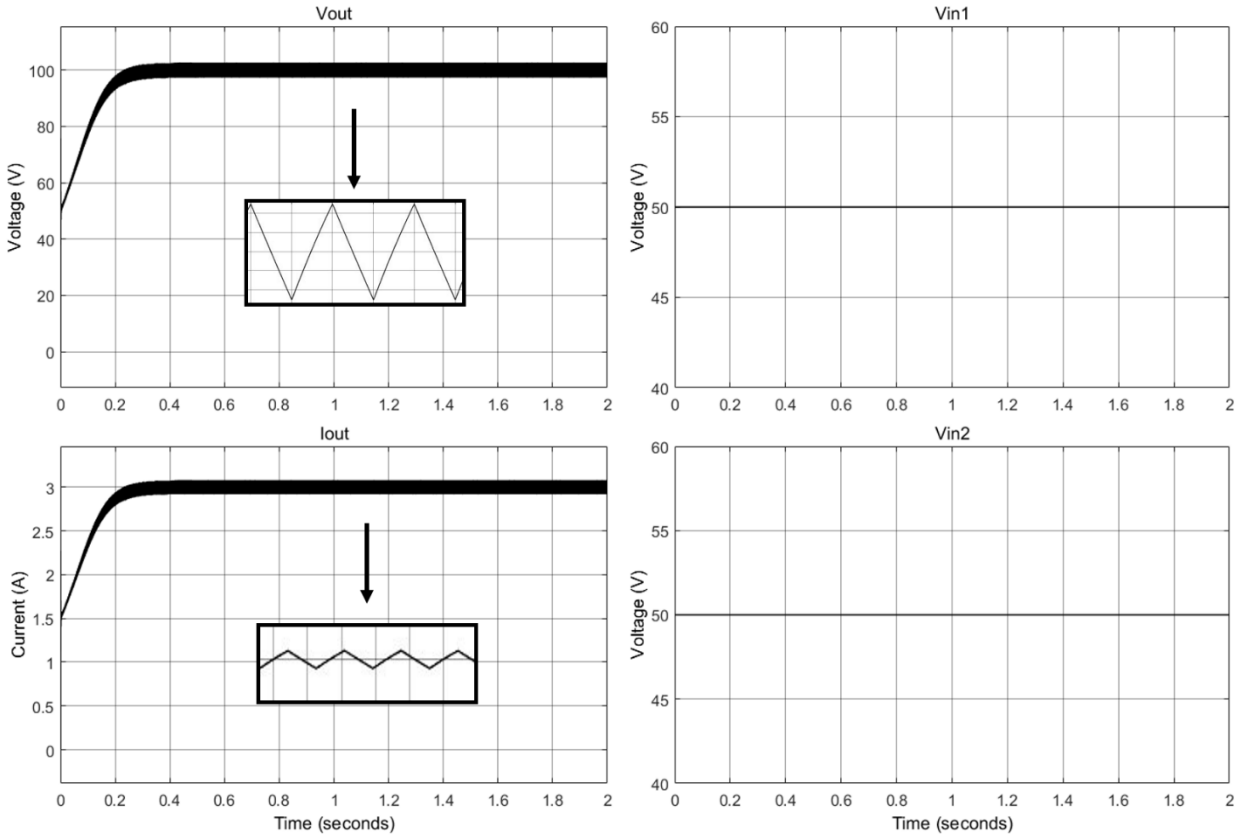

Fig 5.14: Simulation results during the third mode (load)

Figure 5.15 shows the experimental results of the output behavior of the load during the boost stage, and it is typical of the simulation results of the third mode. A DC voltage source V_{in}= 30 V is used. From top to bottom are the waveforms of output voltage V_o, output current I_o and switching commands S_6 and S_1. The switching commands S_6 and S_1 have duty ratios of 0.7 and 1 at switching frequency of 30 KHz respectively.

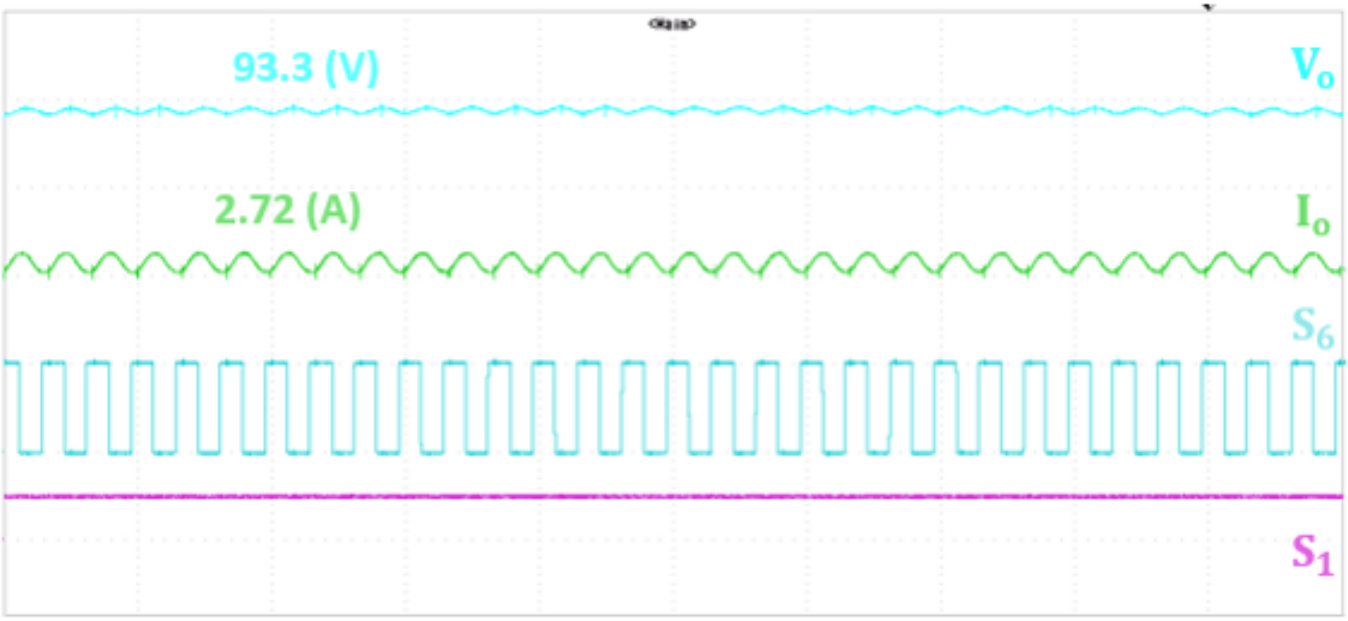

Fig 5.15: Output behavior for Boost stage in Mode III

Figure 5.16 shows the dynamic response of the converter for the second mode with the output behavior of the load and how the controller tune the signal with a fixed settling time (84 ms) according to the variation of the input voltage level:

1) $V_1 = 50$ V

2) $V_1 = 43$ V

3) $V_1 = 25$ V

4) $V_1 = 37$ V

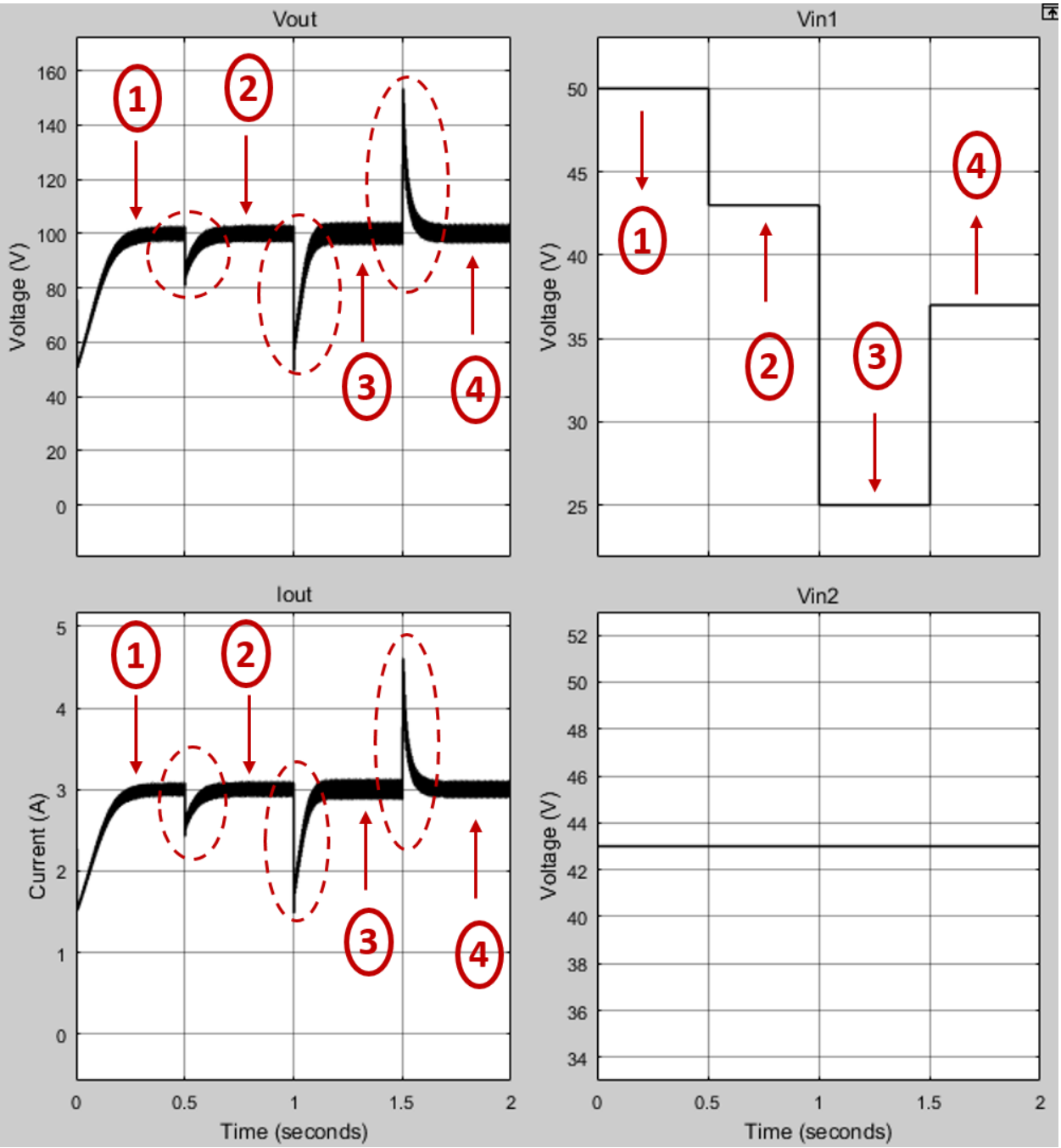

Fig 5.16: Dynamic response during the third mode (load)

Figure 5.17 shows the simulation results of the output behavior of the battery when the SOC of battery reaches 90 %. DC voltage sources V_1= 50 V and V_2= 50 V are used.

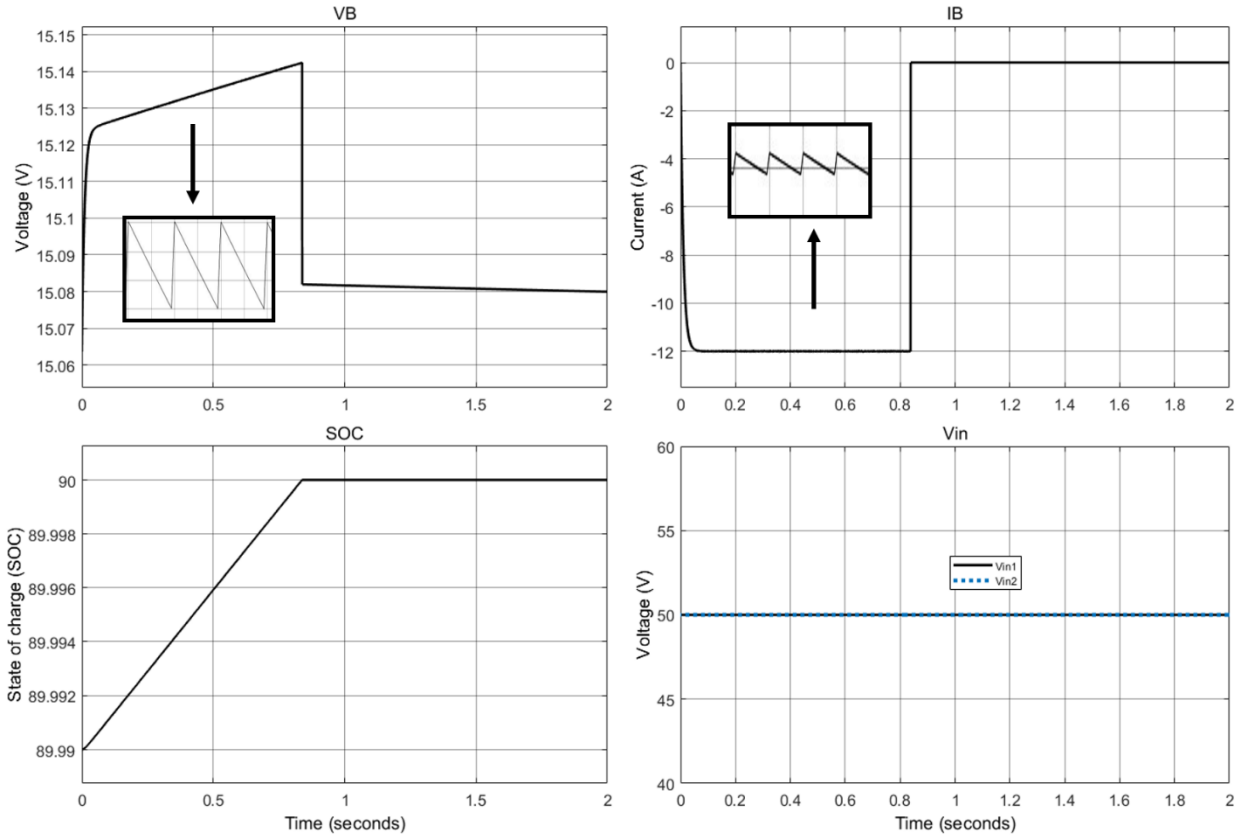

Fig 5.17: Simulation results during the third mode (battery)

4) Load supplying and battery discharging:

As both of the two sources failed to operate, the battery started to supply the load ensuring that the discharging process will stop at 20% and with very low voltage compare to the other modes and with fixed input voltage, showing the required output power, knowing that during this process if the first source V1 was able to operate again the output power will remain the same. Figure 5.18 shows the simulation results of the output behavior of the load during the boost stage. A battery module was selected as a DC source V_3= 15 V is used.

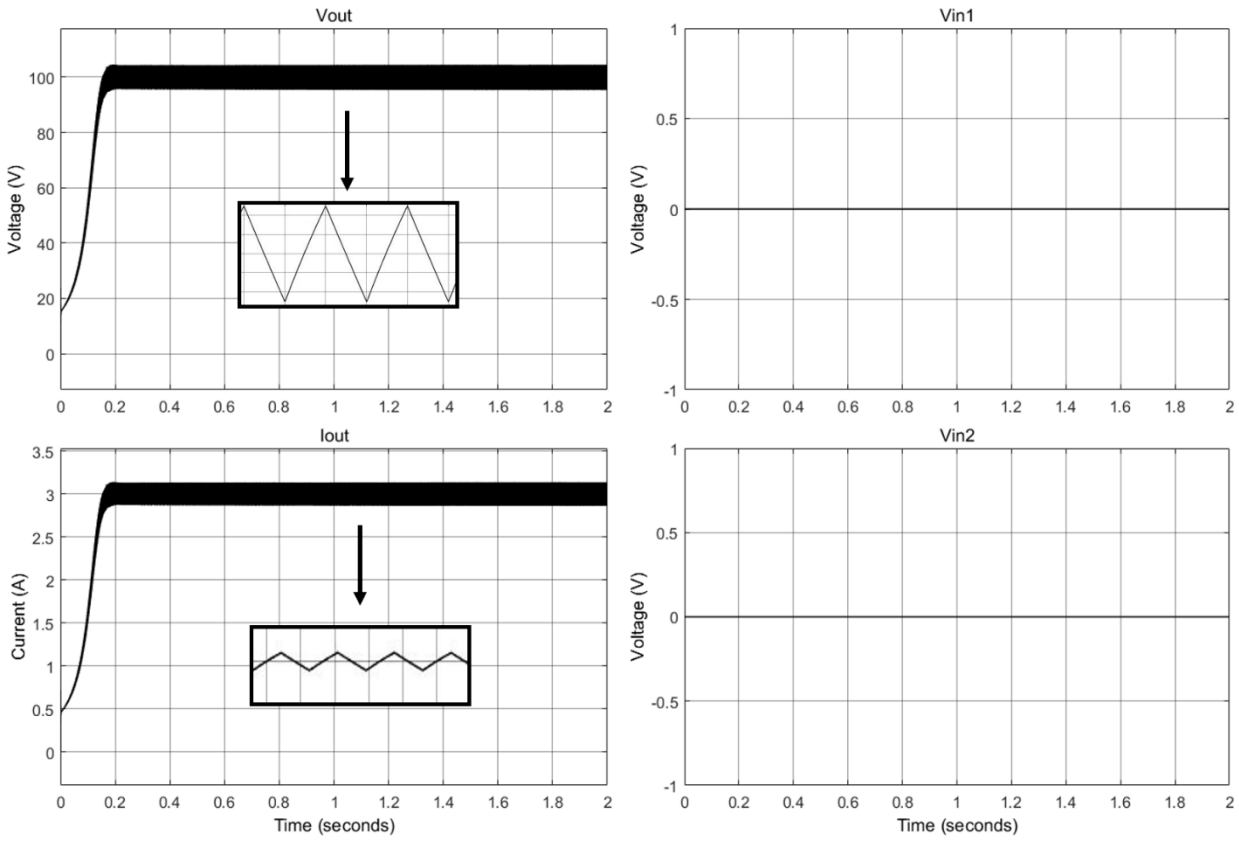

Fig 5.18: Simulation results during the fourth mode (load)

Figure 5.19 shows the experimental results of the output behavior of the load during the boost stage, and it is typical of the simulation results of the fourth mode. A 25 V battery is used to compare the output power value with the first three modes and to show the stability of the converter. From top to bottom are the waveforms of output voltage V_o, output current I_o and switching commands S_5 and S_6. The switching commands S_5 and S_6 have duty ratios of 1 and 0.75 at switching frequency of 30 kHz respectively.

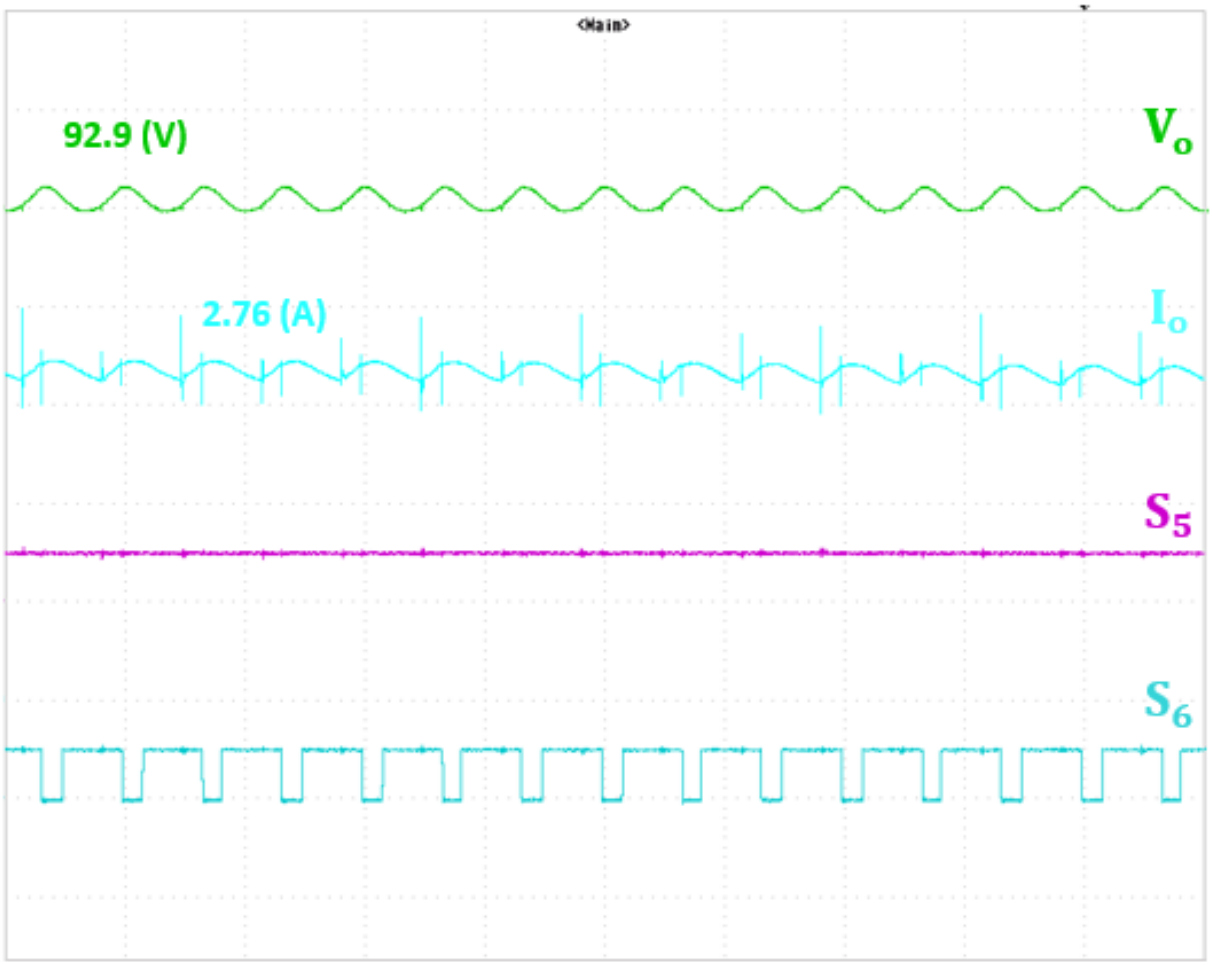

Fig 5.19: Output behavior for Boost stage in Mode IV

Figure 5.20 shows the simulation results of the output behavior of the battery during the discharging process to supply the load. A battery module was selected as a DC source V_3= 15 V is used.

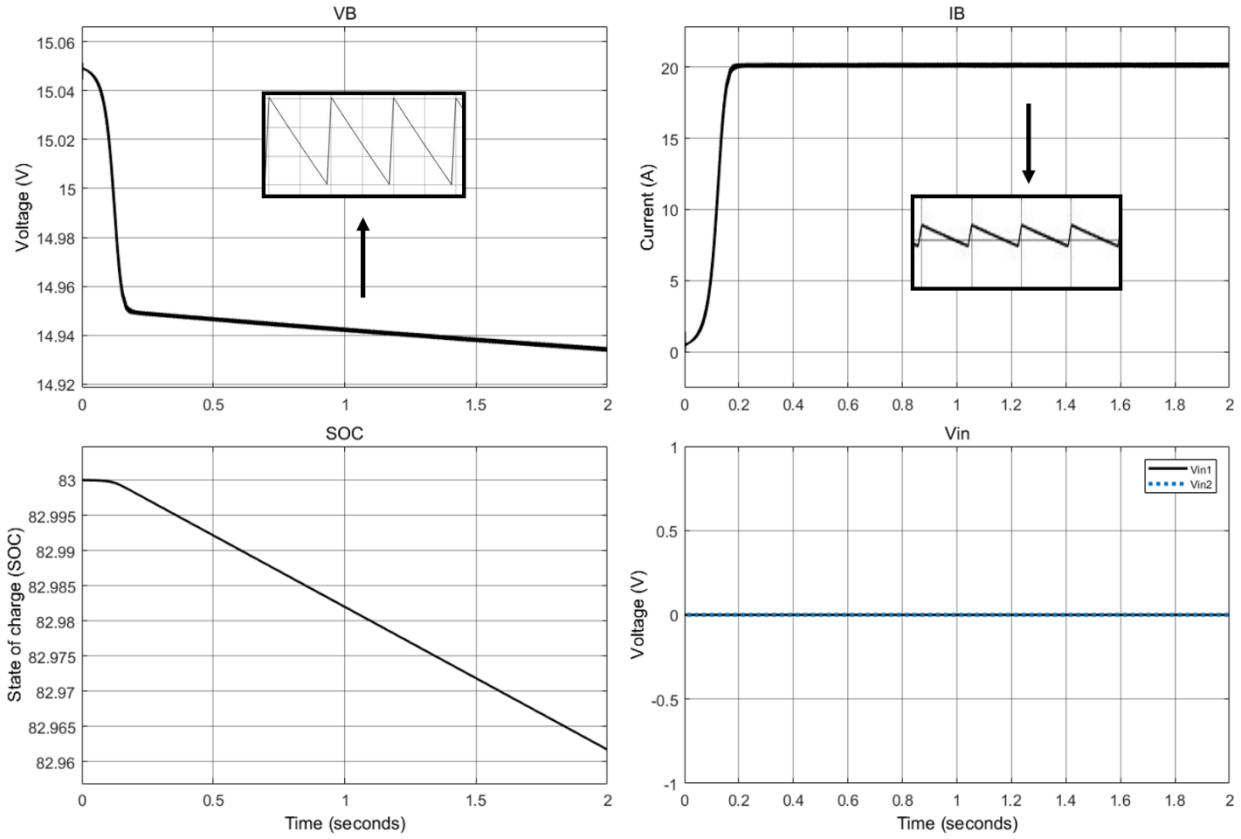

Fig 5.20: Simulation results during the fourth mode (battery)

5.4. Summary

This chapter outlines all the parameters values, all the test equipment, the behavior of the converter in each mode, the test procedures with the relating mode conditions and shows the capability of the converter of supplying constant output power through different input sources with different voltage variation.

The duty ratio is changed according to the input voltage as shown in Figure 5.21 to obtain the desired output power. The converter is operating in all four modes, showing high efficiency and performance and the energy produced from the sources can be charged in the battery as well as discharging the battery to supply the load.

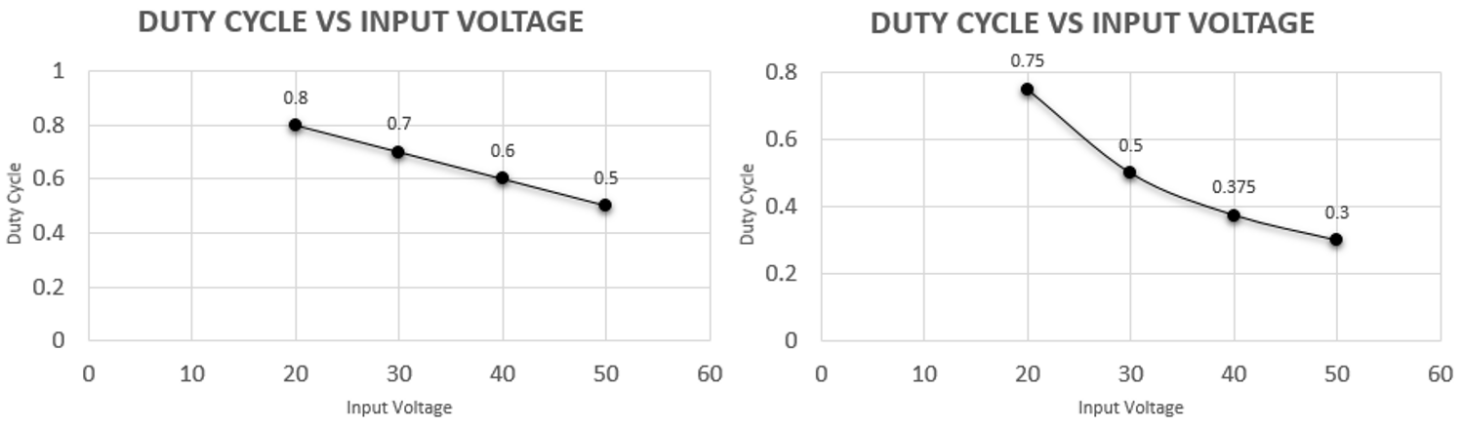

Boost Stage Buck Stage

Fig 5.21: Duty cycle with input voltage variation

Different testing procedures are done to get the efficiency of each mode and the overall performance of the converter. Table 5.4 shows the converter performance according to the input and output power in each mode during the boost and buck stages.

Table 5.4: Converter performance

Operation	Stage	Input power	Output power	Power loss	Efficiency
Mode 1	Boost	285 W	261.52 W	23.48 W	91.76 %
Mode 1	Buck	280 W	255.84 W	24.16 W	91.3 %
Mode 2	Boost	275 W	247.77 W	27.23 W	90 %
Mode 2	Buck	275 W	247.84 W	27.16 W	90.13 %
Mode 3	Boost	285 W	262.08 W	22.92 W	91.95 %
Mode 4	Boost	287.5 W	263.57 W	23.93 W	91.6 %

Figure 5.22 to Figure 5.24 show the efficiency of the converter with the variation of the input voltage in the first three modes. The converter was tested using the different input voltage levels starting from the maximum value to the minimum value.

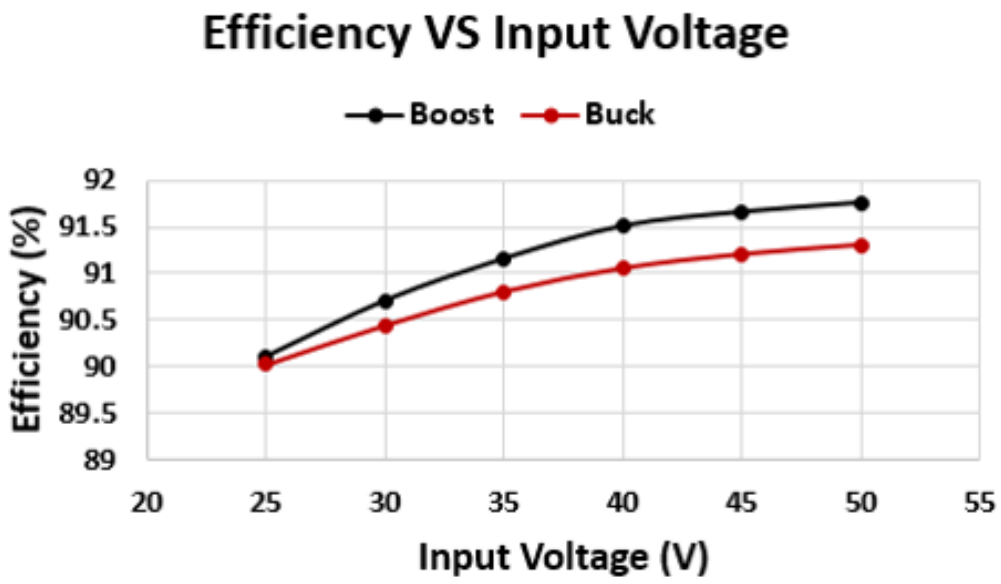

Fig 5.22: Efficiency for Mode I

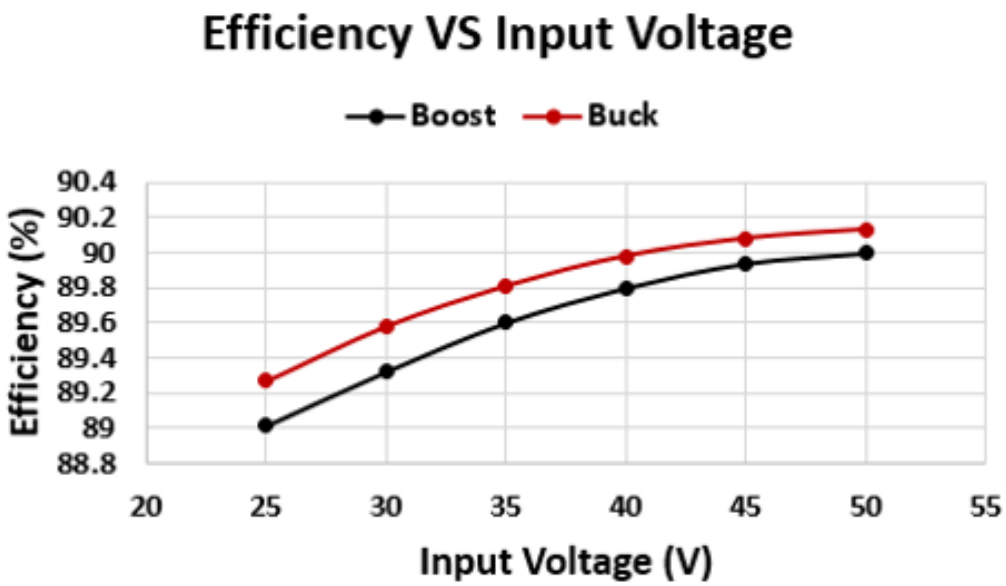

Fig 5.22: Efficiency for Mode II

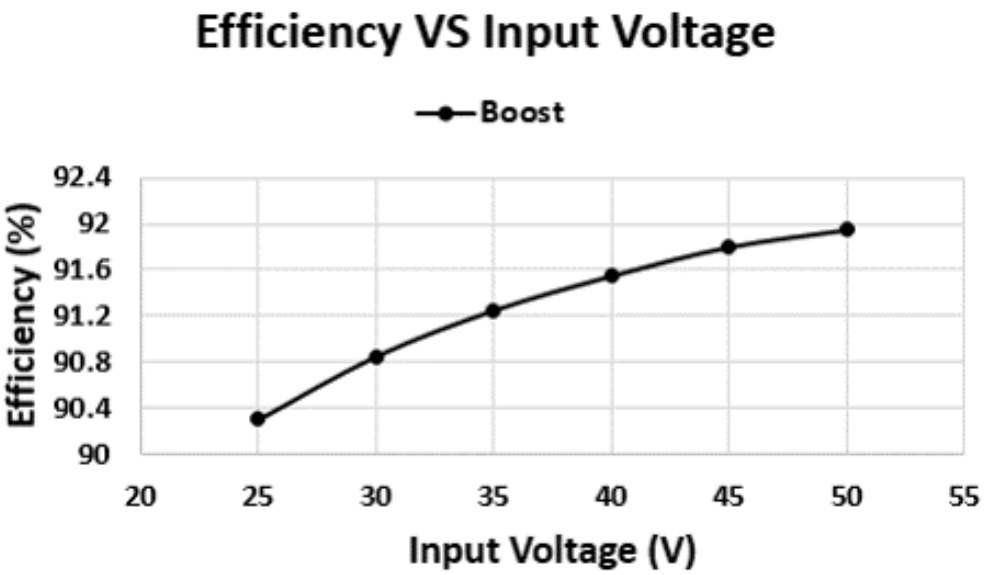

Fig 5.23: Efficiency for Mode III

Chapter 6
Conclusion and Future Work

This thesis proposed a novel structure of multi-input converter for effective renewable energy management, capable of supplying constant output power through different input sources with any voltage variation. Chapter 1 of this thesis provided an introduction on all aspects of DC-DC converters as well as multiple-input DC-DC converters topologies and characteristics. New topologies are introduced to utilize the renewable energy sources and to offer a better solution and structure for different application.

A literature review was done in chapter 2 on some of the existing multiple-input topologies and for the new purposed topologies to make multiple-input converters and their control schemes more efficient and cost effective for integration of renewable energy sources and other applications. The chapter outlines the constraints and challenges to design new topologies.

Chapter 3 discussed the design, operation modes and the control system of the proposed multiple-input converter and the applications for this novel topology.

Chapter 4 provides the background of PV systems, showing the basic structure of the circuit and modules and how it was implemented for the simulation tests. PV systems are selected as they are considered as future energy sources due to their sustainability and environmental friendliness. These sources offer an alternative energy solution to reduce the carbon emissions and have a lot of benefits such as reducing line losses, improving voltage profile, efficiency improvement and power quality improvement.

In chapter 5 the DC sources were implemented as input sources with the converter and all of the parameters were outlined. The simulation procedure of each mode is explained in details, showing the validation and the performance of the converter and the capability of charging the battery and supplying the load at the same time. The results show a high performance and all of the operating modes have been investigated, showing that the topological structure provides an effective renewable energy management. Testing procedures, all of the parameters and the hardware implementation of the converter are outlined. The testing procedure of each mode is explained in details. All of the experimental results are similar to the simulation results which validate the performance of the topology.

6.1. Contribution

- The DC-DC converters and the purpose and advantages of the multi-input converters was studied in the first chapter. The multiple-input converters play avital role to reduce the energy consumption and to improve our energy security as it can be utilized for a lot of assorted applications and can be implemented for the renewable energy applications.

- The advantages and the disadvantages of the various topologies are studied to address the main constraints and introduce an efficient converter focusing on improving the efficiency, size and the cost of the multi input converter and to introduce an effective energy management method of the renewable energy sources.

- A novel multiple-input DC-DC converter was designed to provide a fixed output power with an effective energy management of renewable sources and to

introduce a simpler control algorithm for this converter as it was designed for implementation for different applications standards.

- The converter was simulated for validation with a list of all of the components values and dynamic response of the converter regarding the change of the input voltage levels and to determine the efficiency of each mode and to observe the output behavior of the load and charging and discharging state of the battery. The capability of the converter was tested to supply the load for longer time and to address the advantages of the compact structure of the design.

- A prototype was built with the testing procedure, equipment, and components to confirm the behavior of the converter and its control system. According to the output behavior of the converter, it can be used for different applications and has a high efficiency because of the control algorithm and the compact structure of the design. The topology is used for efficient renewable energy management and it can be improved to introduce more benefits for the industrial area.

6.2. Future Work

- The topology was tested only with DC loads to experimentally verify of the design and the overall efficiency of the converter. A DC-AC inverter for grid application can be added to improve the utilization of the renewable energy sources and to keep the continuous improvement in the industrial areas and to solve the load demand problem as the infirm nature of the clean energy power supply will need a smart grid management at scale.

- Using planar magnetics for inductors for their advantages:

1. Significantly reduced height.
2. Greater surface area, resulting in improved heat dissipation capability.
3. Greater magnetic cross-section area, enabling fewer turns.
4. Lower leakage inductance resulting from fewer turns and interleaved windings.
5. Excellent reproducibility, enabled by winding structure.

- A fast charging method for the battery such as the constant-current charging method and the constant-voltage charging method can be used for better SOC state results to extend the lifetime of the battery and to improve the effectiveness of the charging and discharging techniques. Other alternatives can be used such as energy storage unit and capacitors to improve the SOC characteristics.

- The topology can be modified through two phases:

1. Phase 1 can be designed to get better efficiency, control system and structure by reducing the number of components and implementing an optimized control algorithm.
2. Phase 2 can be designed to have more than two renewable energy sources and to be utilized for different application at the same time depending on the renewable energy management methods.

REFERENCES

[1] G. Zhang, Z. Li, B. Zhang, and W. A. Halang, 'Power electronics converters: Past, present and future', Renew. Sustain. Energy Rev., vol. 81, pp. 2028–2044, Jan. 2018.

[2] S. Sivakumar, M. J. Sathik, P. S. Manoj, and G. Sundararajan, 'An assessment on performance of DC–DC converters for renewable energy applications', Renew. Sustain. Energy Rev., vol. 58, pp. 1475–1485, May 2016.

[3] Z. Rehman, I. Al-Bahadly, and S. Mukhopadhyay, 'Multiinput DC–DC converters in renewable energy applications – An overview', Renew. Sustain. Energy Rev., vol. 41, pp. 521–539, Jan. 2015.

[4] J. Zeng, W. Qiao, L. Qu, and Y. Jiao, 'An Isolated Multiport DC–DC Converter for Simultaneous Power Management of Multiple Different Renewable Energy Sources', IEEE J. Emerg. Sel. Top. Power Electron., vol. 2, no. 1, pp. 70–78, Mar. 2014.

[5] S. Khosrogorji, M. Ahmadian, H. Torkaman, and S. Soori, 'Multi-input DC/DC converters in connection with distributed generation units – A review', Renew. Sustain. Energy Rev., vol. 66, pp. 360–379, Dec. 2016.

[6] J. B. Klaassens, E. Van Dijk, H. J. N. Spruijt, D. M. O'sullivan, and J. Ben Klaassens, 'PWM-switch modeling of DC-DC converters', IEEE Trans. POWER Electron., vol. 10, no. 6, 1995.

[7] W. Li, X. Lv, Y. Deng, J. Liu, and X. He, 'A Review of Non-Isolated High Step-Up DC/DC Converters in Renewable Energy Applications', in 2009 Twenty-Fourth Annual IEEE Applied Power Electronics Conference and Exposition, 2009, pp. 364–369.

[8] M. Forouzesh, Y. P. Siwakoti, S. A. Gorji, F. Blaabjerg, and B. Lehman, 'Step-Up DC–DC Converters: A Comprehensive Review of Voltage-Boosting Techniques, Topologies, and Applications', IEEE Trans. Power Electron., vol. 32, no. 12, pp. 9143–9178, Dec. 2017.

[9] S. J. Finney, G. P. Adam, B. W. Williams, D. Holliday, and I. A. Gowaid, 'Review of dc–dc converters for multi-terminal HVDC transmission networks', IET Power Electron., vol. 9, no. 2, pp. 281–296, Feb. 2016.

[10] H. Matsuo, W. Lin, F. Kurokawa, S. Member, T. Shigemizu, and N. Watanabe, 'Characteristics of the Multiple-Input DC-DC Converter', IEEE Trans. Ind. Electron., vol. 51, no. 3, 2004.

[11] Y. Li, X. Ruan, D. Yang, F. Liu, and C. K. Tse, 'Synthesis of Multiple-Input DC/DC Converters', IEEE Trans. Power Electron., vol. 25, no. 9, pp. 2372–2385, Sep. 2010.

[12] A. Kwasinski, 'Identification of Feasible Topologies for Multiple-Input DC-DC Converters', IEEE Trans. POWER Electron., vol. 24, no. 3, 2009.

[13] K. Varesi, S. H. Hosseini, M. Sabahi, E. Babaei, and N. Vosoughi, 'An improved Non-Isolated Multiple-Input buck dc-dc converter', in 2017 8th Power Electronics, Drive Systems & Technologies Conference (PEDSTC), 2017, pp. 119–124.

[14] S. Ramya, A. Napolean, and T. Manoharan, 'A novel converter topology for stand-alone hybrid PV/Wind/battery power system using Matlab/Simulink', in 2013 International Conference on Power, Energy and Control (ICPEC), 2013, pp. 17–22.

[15] F. Nejabatkhah, S. Danyali, S. H. Hosseini, M. Sabahi, and S. M. Niapour, 'Modeling and Control of a New Three-Input DC–DC Boost Converter for Hybrid PV/FC/Battery Power System', IEEE Trans. Power Electron., vol. 27, no. 5, pp. 2309–2324, May 2012.

[16] S. Khosrogorji, H. Torkaman, and F. Karimi, 'A short review on multi-input DC/DC converters topologies', in The 6th Power Electronics, Drive Systems & Technologies Conference (PEDSTC2015), 2015, pp. 650–654.

[17] N. Vazquez, A. Hernandez, C. Hernandez, E. Rodriguez, and J. Arau, 'Two inputs DC/DC Converter applicable in clean-energy resources', in 2008 11th IEEE International Power Electronics Congress, 2008, pp. 185–189.

[18] K. P. Yalamanchili, M. Ferdowsi, and K. Corzine, 'New Double Input DC-DC Converters for Automotive Applications', in 2006 IEEE Vehicle Power and Propulsion Conference, 2006, pp. 1–6.

[19] S. Athikkal, K. Sundaramoorthy, and A. Sankar, 'Development and performance analysis of dual-input DC-DC converters for DC microgrid application', IEEJ Trans. Electr. Electron. Eng., vol. 13, no. 7, pp. 1034–1043, Jul. 2018.

[20] S. Abdul Hamid, M. Yusof Othman, K. Sopian, and S. H. Zaidi, 'An overview of photovoltaic thermal combination (PV/T combi) technology', *Renew. Sustain. Energy*

Rev., vol. 38, pp. 212–222, Oct. 2014.

[21] S. Kouro, J. I. Leon, D. Vinnikov, and L. G. Franquelo, 'Grid-Connected Photovoltaic Systems: An Overview of Recent Research and Emerging PV Converter Technology', *IEEE Ind. Electron. Mag.*, vol. 9, no. 1, pp. 47–61, Mar. 2015.

[22] Z. Wang and H. Li, 'An Integrated Three-Port Bidirectional DC–DC Converter for PV Application on a DC Distribution System', *IEEE Trans. Power Electron.*, vol. 28, no. 10, pp. 4612–4624, Oct. 2013.

[23] H. AbdEl-Gawad and V. K. Sood, 'Kalman filter-based maximum power point tracking for PV energy resources supplying DC microgrid', in *2017 IEEE Electrical Power and Energy Conference (EPEC)*, 2017, pp. 1–8.

[24] A. Lavanya, J. D. Navamani, K. Vijayakumar, and R. Rakesh, 'Multi-input DC-DC converter topologies-a review', in 2016 International Conference on Electrical, Electronics, and Optimization Techniques (ICEEOT), 2016, pp. 2230–2233.

[25] N. Zhang, D. Sutanto, and K. M. Muttaqi, 'A review of topologies of three-port DC–DC converters for the integration of renewable energy and energy storage system', Renew. Sustain. Energy Rev., vol. 56, pp. 388–401, Apr. 2016.

[26] K. Jyotheeswara Reddy and S. Natarajan, 'Energy sources and multi-input DC-DC converters used in hybrid electric vehicle applications – A review', Int. J. Hydrogen Energy, vol. 43, no. 36, pp. 17387–17408, Sep. 2018.

[27] S. H. Hosseini, S. Danyali, F. Nejabatkhah, and S. A. K. Mozafari Niapoor, 'Multi-input DC boost converter for grid connected hybrid PV/FC/Battery power system', in 2010 IEEE Electrical Power & Energy Conference, 2010, pp. 1–6.

[28] Zhijun Qian, O. Abdel-Rahman, and I. Batarseh, 'An Integrated Four-Port DC/DC Converter for Renewable Energy Applications', IEEE Trans. Power Electron., vol. 25, no. 7, pp. 1877–1887, Jul. 2010.

[29] A. Nahavandi, M. T. Hagh, M. B. B. Sharifian, and S. Danyali, 'A Nonisolated Multiinput Multioutput DC–DC Boost Converter for Electric Vehicle Applications', IEEE Trans. Power Electron., vol. 30, no. 4, pp. 1818–1835, Apr. 2015.

[30] Zhijun Qian, O. Abdel-Rahman, H. Al-Atrash, and I. Batarseh, ‘Modeling and Control of Three-Port DC/DC Converter Interface for Satellite Applications’, IEEE Trans. Power Electron., vol. 25, no. 3, pp. 637–649, Mar. 2010.

[31] S. Athikkal, K. Sundaramoorthy, and A. Sankar, ‘Design, Fabrication and Performance Analysis of a Two Input-Single Output DC-DC Converter’.

[32] M. Suetomi et al., ‘A novel multi-input DC-DC converter with high power efficiency’, in 2011 IEEE 33rd International Telecommunications Energy Conference (INTELEC), 2011, pp. 1–5.

[33] A. Deihimi, M. E. Seyed Mahmoodieh, and R. Iravani, ‘A new multi-input step-up DC–DC converter for hybrid energy systems’, Electr. Power Syst. Res., vol. 149, pp. 111–124, Aug. 2017.

[34] E. Babaei and O. Abbasi, ‘A new topology for bidirectional multi-input multi-output buck direct current-direct current converter’, Int. Trans. Electr. Energy Syst., vol. 27, no. 2, p. e2254, Feb. 2017.

[35] E. Babaei and O. Abbasi, ‘Structure for multi-input multi-output dc–dc boost converter’, IET Power Electron., vol. 9, no. 1, pp. 9–19, Jan. 2016.

[36] P. Mohseni, S. H. Hosseini, M. Sabahi, T. Jalilzadeh, and M. Maalandish, ‘A New High Step-Up Multi-Input Multi-Output DC-DC Converter’, IEEE Trans. Ind. Electron., pp. 1–1, 2018.

[37] P. KhademiAstaneh, J. Javidan, K. Valipour, and A. Akbarimajd, ‘A bidirectional high step-up multi-input DC-DC converter with soft switching’, Int. Trans. Electr. Energy Syst., vol. 29, no. 1, p. e2699, Jan. 2019.

[38] Y.-C. Liu and Y.-M. Chen, ‘A Systematic Approach to Synthesizing Multi-Input DC–DC Converters’, IEEE Trans. Power Electron., vol. 24, no. 1, pp. 116–127, Jan. 2009.

[39] R. R. Ahrabi, H. Ardi, M. Elmi, and A. Ajami, ‘A Novel Step-Up Multiinput DC–DC Converter for Hybrid Electric Vehicles Application’, IEEE Trans. Power Electron., vol. 32, no. 5, pp. 3549–3561, May 2017.

[40] A. Deihimi, M. E. Seyed Mahmoodieh, and R. Iravani, ‘A new multi-input step-up DC–DC converter for hybrid energy systems’, Electr. Power Syst. Res., vol. 149, pp. 111–124, Aug. 2017.

[41] S. Athikkal, K. Sundaramoorthy, and A. Sankar, ‘A Modified Dual Input DC-DC Converter for Hybrid Energy Application’, Int. J. Power Electron. Drive Syst., vol. 8, no. 1, pp. 81–92, 2017.

[42] C. Balaji, S. S. Dash, N. Hari, and P. C. Babu, ‘A four port non-isolated multi input single output DC-DC converter fed induction motor’, in 2017 IEEE 6th International Conference on Renewable Energy Research and Applications (ICRERA), 2017, pp. 631–637.

[43] A. Lavanya, K. Vijaya Kumar, and J. D. Navamani, ‘Topological Comparison of Dual-Input DC-DC Converters’, Int. J. Power Electron. Drive Syst., vol. 8, no. 2, pp. 804–811, 2017.

[44] S. Moury and J. Lam, ‘New soft-switched high frequency multi-input step-up/down converters for high voltage DC-distributed hybrid renewable systems’, in 2017 IEEE Energy Conversion Congress and Exposition (ECCE), 2017, pp. 5537–5544.

[45] K. Varesi, S. H. Hosseini, M. Sabahi, E. Babaei, and N. Vosoughi, ‘An improved Non-Isolated Multiple-Input buck dc-dc converter’, in 2017 8th Power Electronics, Drive Systems & Technologies Conference (PEDSTC), 2017, pp. 119–124.

[46] F. Kardan, R. Alizadeh, and M. R. Banaei, ‘A New Three Input DC/DC Converter for Hybrid PV/FC/Battery Applications’, IEEE J. Emerg. Sel. Top. Power Electron., vol. 5, no. 4, pp. 1771–1778, Dec. 2017.

[47] F. L. Luo, H. Ye, and H. Ye, Power Electronics. CRC Press, 2018.

[48] M. Kazmierkowski, ‘Power converters and amplifiers (review of "Pulse-Width Modulated DC-DC Power Converters" by Kazimierczuk, M.K.; 2008) [Book News’, IEEE Ind. Electron. Mag., vol. 3, no. 2, pp. 44–44, Jun. 2009.

[49] N. Ahmadian, A. Khosravi, and P. Sarhadi, ‘A New Approach to Adaptive Control of Multi-Input Multi-Output Systems Using Multiple Models’, J. Dyn. Syst. Meas. Control, vol. 137, no. 9, p. 091009, Sep. 2015.

[50] E. B. Kosmatopoulos and P. A. Ioannou, ‘Robust switching adaptive control of multi-input nonlinear systems’, IEEE Trans. Automat. Contr., vol. 47, no. 4, pp. 610–624, Apr. 2002.

[51] Q.-F. Liao, D. Sun, W.-J. Cai, S.-Y. Li, and Y.-Y. Wang, ‘Type-1 and Type-2 effective Takagi-Sugeno fuzzy models for decentralized control of multi-input-multi-output processes’, J. Process Control, vol. 52, pp. 26–44, Apr. 2017.

[52] O. Lopez-Lapena, ‘Time-Division Multiplexing Control of Multi-Input Converters for Low-Power Solar Energy Harvesters’, IEEE Trans. Ind. Electron., vol. 65, no. 12, pp. 9668–9676, Dec. 2018.

[53] W. Chen, X. Ruan, H. Yan, and C. K. Tse, ‘DC/DC Conversion Systems Consisting of Multiple Converter Modules: Stability, Control, and Experimental Verifications’, IEEE Trans. Power Electron., vol. 24, no. 6, pp. 1463–1474, Jun. 2009.

[54] Huang-Jen Chiu, Hsiu-Ming Huang, Li-Wei Lin, and Ming-Hsiang Tseng, ‘A Multiple-Input DC/DC Converter for Renewable Energy Systems’, in 2005 IEEE International Conference on Industrial Technology, pp. 1304–1308.

[55] S. H. Choung and A. Kwasinski, ‘Multiple-input DC-DC converter topologies comparison’, in 2008 34th Annual Conference of IEEE Industrial Electronics, 2008, pp. 2359–2364.

[56] F. Nejabatkhah, S. Danyali, S. H. Hosseini, M. Sabahi, and S. M. Niapour, ‘Modeling and Control of a New Three-Input DC–DC Boost Converter for Hybrid PV/FC/Battery Power System’, IEEE Trans. Power Electron., vol. 27, no. 5, pp. 2309–2324, May 2012.

[57] L. Solero, A. Lidozzi, and J. A. Pomilio, ‘Design of Multiple-Input Power Converter for Hybrid Vehicles’, IEEE Trans. Power Electron., vol. 20, no. 5, pp. 1007–1016, Sep. 2005.

[58] Y.-M. Chen, Y.-C. Liu, F.-Y. Wu, and T.-F. Wu, ‘Multi-input DC/DC converter based on the flux additivity’, in Conference Record of the 2001 IEEE Industry Applications Conference. 36th IAS Annual Meeting (Cat. No.01CH37248), vol. 3, pp. 1866–1873.

[59] N. D. Benavides, T. Esram, and P. L. Chapman, ‘Ripple Correlation Control of a Multiple-Input Dc-Dc Converter’, in IEEE 36th Conference on Power Electronics Specialists, 2005., pp. 160–164.

[60] F. Akar, Y. Tavlasoglu, E. Ugur, B. Vural, and I. Aksoy, 'A Bidirectional Nonisolated Multi-Input DC–DC Converter for Hybrid Energy Storage Systems in Electric Vehicles', IEEE Trans. Veh. Technol., vol. 65, no. 10, pp. 7944–7955, Oct. 2016.

[61] H. Behjati and A. Davoudi, 'A Multiple-Input Multiple-Output DC–DC Converter', IEEE Trans. Ind. Appl., vol. 49, no. 3, pp. 1464–1479, May 2013.

[62] A. K. Bhattacharjee, N. Kutkut, and I. Batarseh, 'Review of Multiport Converters for Solar and Energy Storage Integration', IEEE Trans. Power Electron., vol. 34, no. 2, pp. 1431–1445, Feb. 2019.

[63] S. Athikkal, K. Sundaramoorthy, and A. Sankar, 'Development and performance analysis of dual-input DC-DC converters for DC microgrid application', IEEJ Trans. Electr. Electron. Eng., vol. 13, no. 7, pp. 1034–1043, Jul. 2018.

[64] K. Jyotheeswara Reddy and S. Natarajan, 'Energy sources and multi-input DC-DC converters used in hybrid electric vehicle applications – A review', Int. J. Hydrogen Energy, vol. 43, no. 36, pp. 17387–17408, Sep. 2018.

[65] S. Athikkal, K. Sundaramoorthy, and A. Sankar, 'A Modified Dual Input DC-DC Converter for Hybrid Energy Application', Int. J. Power Electron. Drive Syst., vol. 8, no. 1, pp. 81–92, 2017.

[66] A. Lavanya, K. Vijaya Kumar, and J. D. Navamani, 'Topological Comparison of Dual-Input DC-DC Converters', Int. J. Power Electron. Drive Syst., vol. 8, no. 2, pp. 804–811, 2017.

[67] V. Karthikeyan and R. Gupta, 'Multiple-Input Configuration of Isolated Bidirectional DC–DC Converter for Power Flow Control in Combinational Battery Storage', IEEE Trans. Ind. Informatics, vol. 14, no. 1, pp. 2–11, Jan. 2018.

[68] F. Ahmad, A. A. Haider, H. Naveed, A. Mustafa, and I. Ahmad, 'Multiple Input Multiple Output DC to DC Converter', in 2018 5th International Multi-Topic ICT Conference (IMTIC), 2018, pp. 1–6.

[69] C. Kallukaran, L. Unnikrishnan, and R. A. Koshy, 'Multi-Input Interleaved DC-DC Converter with Low Current Ripple for Electric Vehicle Application', in 2018 International Conference on Current Trends towards Converging Technologies (ICCTCT), 2018, pp. 1–5.

[70] G. Lara-Salazar, N. Vazquez, C. Hernandez, H. Lopez, and J. Arau, ‘Multi-input DC/DC converter with battery backup for renewable applications’, in 2016 13th International Conference on Power Electronics (CIEP), 2016, pp. 47–51.

[71] [N. Zhang, D. Sutanto, and K. M. Muttaqi, ‘A buck-boost converter based multi-input DC-DC/AC converter’, in 2016 IEEE International Conference on Power System Technology (POWERCON), 2016, pp. 1–6.

Appendix A

MATLAB: Battery Module Graph

Battery discharge characteristic